Contents

Chapter 16

Waves

Version 1216.2.K, 9 June 2013 *Please send comments, suggestions, and errata via email to kip@caltech.edu or on paper to Kip Thorne, 350-17 Caltech, Pasadena CA 91125*

Box 16.1
Reader's Guide

- This chapter relies heavily on Chaps. 13 and 14, and less heavily on geometric-optics concepts introduced in Secs. 7.2 and 7.3.

- Chap. 17 (compressible flows) relies to some extent on Secs. 16.2, 16.3 and 16.5 of this chapter.

- Sec. 16.3 on solitons on water is a foundation for Sec. 23.6 on solitons in plasmas.

- The remaining chapters of this book do not rely significantly on this chapter.

16.1 Overview

In the preceding chapters, we have derived the basic equations of fluid dynamics and developed a variety of techniques to describe stationary flows. We have also demonstrated how, even if there exists a rigorous, stationary solution of these equations for a time-steady flow, instabilities may develop, in which the amplitude of an oscillatory disturbance grows with time. These unstable modes of an unstable flow can usually be thought of as waves that interact strongly with the flow and extract energy from it. Waves, though, are quite general and can be studied independently of their sources.

Fluid dynamical waves come in a wide variety of forms. They can be driven by a combination of gravitational, pressure, rotational and surface-tension stresses and also by mechanical disturbances, such as water rushing past a boat or air passing through a larynx. In this chapter, we shall describe a few examples of wave modes in fluids, chosen to illustrate general wave properties.

The most familiar types of wave are probably *gravity waves* on the surface of a large body of water (Sec. 16.2), e.g. ocean waves and waves on lakes and rivers. We consider these in the linear approximation and find that they are dispersive in general, though they become nondispersive in the long-wavelength (shallow-water) limit, i.e., when they can feel the water's bottom. We shall illustrate gravity waves by their roles in *helioseismology*, the study of coherent-wave modes excited within the body of the sun by convective overturning motions. We shall also examine the effects of surface tension on gravity waves, which converts them into *capillary waves*, and in this connection shall develop a mathematical description of surface tension (Box 16.4).

In contrast to the elastodynamic waves of Chap. 12, waves in fluids often develop amplitudes large enough that nonlinear effects become important (Sec. 16.3). The nonlinearities can cause the front of a wave to steepen and then break—a phenomenon we have all seen at the sea shore. It turns out that, at least under some restrictive conditions, nonlinear waves have very surprising properties. There exist *soliton* or *solitary-wave* modes in which the front-steepening due to nonlinearity is stably held in check by dispersion, so particular wave profiles are quite robust and propagate for long intervals of time without breaking or dispersing. We shall demonstrate this by studying flow in a shallow channel. We shall also explore the remarkable behaviors of such solitons when they pass through each other.

In a nearly rigidly rotating fluid, there are remarkable waves in which the restoring force is the Coriolis effect, and which have the unusual property that their group and phase velocities are oppositely directed. These so-called *Rossby waves*, studied in Sec. 16.4, are important in both the oceans and the atmosphere.

The simplest fluid waves of all are small-amplitude *sound waves*—a paradigm for scalar waves. These are nondispersive, just like electromagnetic waves, and are therefore sometimes useful for human communication. We shall study sound waves in Sec.16.5 and shall use them to explore (i) the radiation reaction force that acts back on a wave-emitting object (a fundamental physics issue), and (ii) matched asymptotic expansions (a mathematical physics technique). We shall also describe how sound waves can be produced by fluid flows. This will be illustrated with the problem of sound generation by high-speed turbulent flows—a problem that provides a good starting point for the topic of the following chapter, compressible flows.

Other examples of fluid waves are treated elsewhere in Part V: *internal waves* at the interface between two fluids that move relative to each other (Sec. 14.6); *Tollmein-Schlicting waves* in a laminar boundary layer (Ex. 15.10); *lee waves* in a separated boundary layer (footnote 6 in Chap. 15); *wavy Taylor rolls* in rotating Couette flow (Sec. 15.6.1); *shock waves* (Sec. 17.5); *Sedov-Taylor blast waves* (Sec. 17.6); *hydraulic jumps* (Ex. 17.7); and various types of magnetohydrodynamic waves (Chap. 19)

As in Chaps. 14 and 15, readers are urged to watch movies in parallel with reading this chapter; see Box 16.2.

Box 16.2
Movies Relevant to this Chapter
We strongly recommend that the reader view the following movies dealing with waves:

- *Waves in Fluids*, by A. E. Bryson (196?), film in the series by the National Committee for Fluid Mechanics Films, available in 2012 at `http://web.mit.edu/hml/ncfmf.html` .

- *Rotating Flows*, by Dave Fultz (1969); also at `http://web.mit.edu/hml/ncfmf.html` – relevant to Rossby waves, Sec. 16.4.

- *Fluid Motion in a Gravitational Field*, by Hunter Rouse (196?), available in 2012 at `http://www.iihr.uiowa.edu/research/publications-and-media/films-by-hunter-rouse/` – relevant to gravity waves on the surface of water, Sec. 16.2.

16.2   Gravity Waves on the Surface of a Fluid

Gravity waves[1] are waves on and beneath the surface of a fluid, for which the restoring force is the downward pull of gravity. Familiar examples are ocean waves and the waves produced on the surface of a pond when a pebble is thrown in. Less familiar examples are "g-modes" of vibration of the sun, discussed at the end of this section.

Consider a small-amplitude wave propagating along the surface of a flat-bottomed lake with depth h_o, as shown in Fig. 16.1. As the water's displacement is small, we can describe

---

[1]Not to be confused with *gravitational waves,* which are waves in the relativistic gravitational field (spacetime curvature) that propagate at the speed of light, and which we shall meet in Chap. 27.
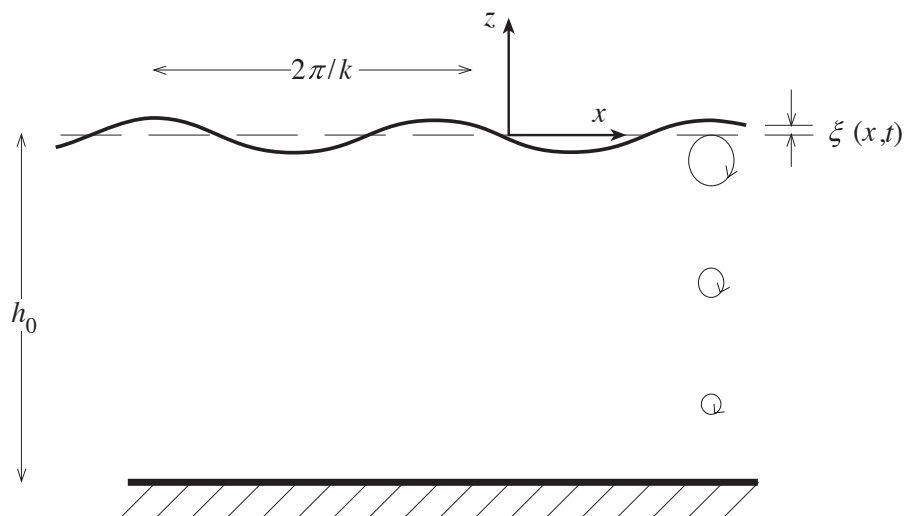

Fig. 16.1: Gravity waves propagating horizontally across a lake with constant depth h_o.

the wave as a linear perturbation about equilibrium. The equilibrium water is at rest, i.e. it has velocity $\mathbf{v} = 0$. The water's perturbed motion is essentially inviscid and incompressible, so $\boldsymbol{\nabla} \cdot \mathbf{v} = 0$. A simple application of the equation of vorticity transport, Eq. (14.3), assures us that, since the water is static and thus irrotational before and after the wave passes, it must also be irrotational within the wave. Therefore, we can describe the wave inside the water by a velocity potential ψ whose gradient is the velocity field,

$$\mathbf{v} = \boldsymbol{\nabla}\psi \, . \tag{16.1}$$

Incompressibility, $\boldsymbol{\nabla} \cdot \mathbf{v} = 0$, applied to this equation, implies that ψ satisfies Laplace's equation

$$\nabla^2 \psi = 0 \, . \tag{16.2}$$

We introduce horizontal coordinates x, y and a vertical coordinate z measured upward from the lake's equilibrium surface (cf. Fig. 16.1), and for simplicity we confine attention to a sinusoidal wave propagating in the x direction with angular frequency ω and wave number k. Then ψ and all other perturbed quantities have the form $f(z) \exp[i(kx - \omega t)]$ for some function $f(z)$. More general disturbances can be expressed as a superposition of many of these elementary wave modes propagating in various horizontal directions (and in the limit, as a Fourier integral over modes). All of the properties of such superpositions follow straightforwardly from those of our elementary plane-wave mode (see Secs. 7.2.2 and 7.3), so we shall continue to focus on it.

We can use Laplace'e equation (16.2) to solve for the vertical variation, $f(z)$, of the velocity potential. As the horizontal variation at a particular time is $\propto \exp(ikx)$, direct substitution into Eq. (16.2) gives two possible vertical variations, $\psi \propto \exp(\pm kz)$. The precise linear combination of these two forms is dictated by the boundary conditions. The one that we shall need is that the vertical component of velocity $v_z = \partial \psi / \partial z$ vanish at the bottom of the lake ($z = -h_o$). The only combination that can vanish is a sinh function. Its integral, the velocity potential, therefore involves a cosh function:

$$\psi = \psi_0 \cosh[k(z + h_o)] \exp[i(kx - \omega t)]. \tag{16.3}$$

An alert reader might note at this point that, for this ψ, the *horizontal* component of velocity $v_x = \psi_{,x} = ik\psi$ does *not* vanish at the lake bottom, in violation of the no-slip boundary condition. In fact, as we discussed in Sec 14.4, a thin, viscous boundary layer along the bottom of the lake will join our potential-flow solution (16.3) to nonslipping fluid at the bottom. We shall ignore the boundary layer under the (justifiable) assumption that for our oscillating waves it is too thin to affect much of the flow.

Returning to the potential flow, we must also impose a boundary condition at the surface. This can be obtained from Bernoulli's law. The version of Bernoulli's law that we need is that for an irrotational, isentropic, time-varying flow:

$$\mathbf{v}^2/2 + h + \Phi + \partial\psi/\partial t = \text{constant everywhere in the flow} \tag{16.4}$$

[Eqs. (13.51), (13.54)]. We shall apply this law at the surface of the perturbed water. Let us examine each term: (i) The term $\mathbf{v}^2/2$ is quadratic in a perturbed quantity and therefore

can be dropped. (ii) The enthalpy $h = u + P/\rho$ (cf. Box 12.1) is a constant since u and ρ are constants throughout the fluid and P is constant on the surface (equal to the atmospheric pressure). [Actually, there will be a slight variation of the surface pressure caused by the varying weight of the air above the surface, but as the density of air is typically $\sim 10^{-3}$ that of water, this is a very small correction.] (iii) The gravitational potential at the fluid surface is $\Phi = g\xi$, where $\xi(x, t)$ is the surface's vertical displacement from equilibrium and we ignore an additive constant. (iv) The constant on the right hand side, which could depend on time $C(t)$, can be absorbed into the velocity potential term $\partial\psi/\partial t$ without changing the physical observable $\mathbf{v} = \boldsymbol{\nabla}\psi$. Bernoulli's law applied at the surface therefore simplifies to give

$$g\xi + \frac{\partial\psi}{\partial t} = 0 . \tag{16.5}$$

Now, the vertical component of the surface velocity in the linear approximation is just $v_z(z = 0, t) = \partial\xi/\partial t$. Expressing v_z in terms of the velocity potential we then obtain

$$\frac{\partial\xi}{\partial t} = v_z = \frac{\partial\psi}{\partial z} . \tag{16.6}$$

Combining this with the time derivative of Eq. (16.5), we obtain an equation for the vertical gradient of ψ in terms of its time derivative:

$$g\frac{\partial\psi}{\partial z} = -\frac{\partial^2\psi}{\partial t^2} . \tag{16.7}$$

Finally, substituting Eq. (16.3) into Eq. (16.7) and setting $z = 0$ [because we derived Eq. (16.7) only at the water's surface], we obtain the dispersion relation[2] for linearized gravity waves:

$$\boxed{\omega^2 = gk\tanh(kh_o)} . \tag{16.8}$$

How do the individual elements of fluid move in a gravity wave? We can answer this question (Ex. 16.1) by computing the vertical and horizontal components of the velocity $v_x = \psi_{,x}$, $v_z = \psi_{,z}$ with ψ given by Eq. (16.3). We find that the fluid elements undergo forward rotating elliptical motion, as depicted in Fig. 16.1, similar to that for Rayleigh waves on the surface of a solid (Sec. 12.4). However, in gravity waves, the sense of rotation is the same (forward) at all depths, in contrast to reversals with depth found in Rayleigh waves; cf. the discussion following Eq. (12.62).

We now consider two limiting cases: deep water and shallow water.

16.2.1 Deep Water Waves — and their Excitation and Damping

When the water is deep compared to the wavelength of the waves, $kh_o \gg 1$, the dispersion relation (16.8) becomes

$$\boxed{\omega = \sqrt{gk}} . \tag{16.9}$$

---

[2]For discussion of dispersion relation, phase velocity, and group velocity for waves, see Sec. 7.2.

Thus, deep water waves are dispersive;[2] their group velocity $V_g \equiv d\omega/dk = \frac{1}{2}\sqrt{g/k}$ is half their phase velocity, $V_\phi \equiv \omega/k = \sqrt{g/k}$. [Note: We could have deduced the deep-water dispersion relation (16.9), up to a dimensionless multiplicative constant, by dimensional arguments: The only frequency that can be constructed from the relevant variables g, k, ρ is $\sqrt{gk}$.]

The quintessential example of deep water waves is waves on an ocean or a lake before they near the shore, so the water's depth is much greater than their wavelength. Such waves, of course, are excited by wind. We have discussed this excitation in Sec. 14.6.2. There we found that the Kelvin-Helmholtz instability (where air flowing in a laminar fashion over water would raise waves) is strongly suppressed by gravity, so this mechanism does not work. Instead, the excitation is by a turbulent wind's randomly fluctuating pressures pounding on the water's surface.

Once the waves have been generated, they can propagate great distances before viscous dissipation damps them; see Ex. 16.2.

16.2.2 Shallow Water Waves

For shallow water waves, with $kh_o \ll 1$, the dispersion relation (16.8) becomes

$$\boxed{\omega = \sqrt{gh_o}\, k} \ . \tag{16.10}$$

Thus, these waves are nondispersive; their phase and group velocities are $V_\phi = V_g = \sqrt{gh_o}$.

Below, when studying solitons, we shall need two special properties of shallow water waves. First, when the depth of the water is small compared with the wavelength, but not very small, the waves will be slightly dispersive. We can obtain a correction to Eq. (16.10) by expanding the tanh function of Eq. (16.8) as $\tanh x = x - x^3/3 + \ldots$. The dispersion relation then becomes

$$\omega = \sqrt{gh_o}\left(1 - \frac{1}{6}k^2 h_o^2\right)k \ . \tag{16.11}$$

Second, by computing $\mathbf{v} = \boldsymbol{\nabla}\psi$ from Eq. (16.3), we find that *in the shallow-water limit the water's horizontal motions are much larger than the vertical motions, and are essentially independent of depth.* The reason, physically, is that the fluid acceleration is produced almost entirely by a horizontal pressure gradient (caused by spatially variable water depth) that is independent of height; see Ex. 16.1.

Often shallow-water waves have heights ξ that are comparable to the water's undisturbed depth h_o, and h_o changes substantially from one region of the flow to another. A familiar example is an ocean wave nearing a beach. In such cases, the wave equation is modified by nonlinear and height-dependent effects. In Box 16.3 we derive the equations that govern such waves, and in Exs. 16.3 and 16.8 and Sec. 16.3 below we explore properties of these waves.

****

EXERCISES

Exercise 16.1 *Example: Fluid Motions in Gravity Waves*

Box 16.3
Nonlinear Shallow-Water Waves with Variable Depth

Consider a nonlinear shallow-water wave propagating on a body of water with variable depth. Let $h_o(x,y)$ be the depth of the undisturbed water at location (x,y) and let $\xi(x,y,t)$ be the height of the wave, so the depth of the water in the presence of the wave is $h = h_o + \xi$. As in the linear-wave case, so also here, the transverse fluid velocity (v_x, v_y) inside the water is nearly independent of height z, so the wave is characterized by three functions $\xi(x,y,t)$, $v_x(x,y,t)$ and $v_y(x,y,t)$. These functions are governed by the law of mass conservation and the inviscid Navier Stokes equation (Euler equation).

The mass per unit area is $\rho h = \rho(h_o + \xi)$ and the corresponding mass flux (mass crossing a unit length per unit time) is $\rho h \mathbf{v} = \rho(h_o + \xi)\mathbf{v}$, where $\mathbf{v}$ is the *2-dimensional, horizontal vectorial velocity* $\mathbf{v} = v_x \mathbf{e}_x + v_y \mathbf{v}_y$. Mass conservation, then, says that $\partial[\rho(h_o + \xi)]/\partial t + {}^{(2)}\boldsymbol{\nabla} \cdot [\rho(h_o + \xi)\mathbf{v}] = 0$, where ${}^{(2)}\boldsymbol{\nabla}$ is the 2-dimensional gradient operator that acts solely in the horizontal (x,y) plane. Since ρ is constant and h_o is time independent, this becomes

$$\partial\xi/\partial t + {}^{(2)}\boldsymbol{\nabla} \cdot [(h_o + \xi)\mathbf{v}] = 0 . \tag{1a}$$

The Navier Stokes equation for $\mathbf{v}$ at an arbitrary height z in the water says $\partial\mathbf{v}/\partial t + (\mathbf{v} \cdot {}^{(2)}\boldsymbol{\nabla})\mathbf{v} = -(1/\rho)\,{}^{(2)}\boldsymbol{\nabla}P$, and hydrostatic equilibrium says the pressure is the weight per unit area of the overlying water, $P = g(\xi - z)\rho$ (where height z is measured from the water's undisturbed surface). Combining these equations we obtain

$$\partial\mathbf{v}/\partial t + (\mathbf{v} \cdot {}^{(2)}\boldsymbol{\nabla})\mathbf{v} + g\,{}^{(2)}\boldsymbol{\nabla} \cdot \xi = 0 . \tag{1b}$$

Equations (1) are used, for example, in theoretical analyses of tsunamis (Ex. 16.3).

(a) Show that in a gravity wave in water of arbitrary depth (deep, shallow, or in between), each fluid element undergoes elliptical motion. (Assume that the amplitude of the water's displacement is small compared to a wavelength.)

(b) Calculate the longitudinal diameter of the motion's ellipse, and the ratio of vertical to longitudinal diameters, as functions of depth.

(c) Show that for a deep-water wave, $kh_o \gg 1$, the ellipses are all circles with diameters that die out exponentially with depth.

(d) We normally think of a circular motion of fluid as entailing vorticity, but a gravity wave in water has vanishing vorticity. How can this vanishing vorticity be compatible with the circular motion of fluid elements?

(e) Show that for a shallow-water wave, $kh_o \ll 1$, the motion is (nearly) horizontal and independent of height z.

(f) Compute the fluid's pressure perturbation $\delta P(x, z, t)$ inside the fluid for arbitrary depth. Show that, for a shallow-water wave the pressure is determined by the need to balance the weight of the overlying fluid, but for general depth, vertical fluid accelerations alter this condition of weight balance.

Exercise 16.2 *Problem: Viscous Damping of Deep Water Waves*

(a) Show that viscosity damps a monochromatic deep water wave with an amplitude e-folding time $\tau_* = (2\nu k^2)^{-1}$, where k is the wave number and ν is the kinematic viscosity. [Hint: Compute the energy E in the wave and the rate of loss of energy to viscous heating $\dot{E}$, and argue that $\tau_* = 2\dot{E}/E$. Recall the discussions of energy in Sec. 13.5.5 and viscous heating in Sec. 13.7.4.]

(b) As an example, consider the ocean waves that one sees at an ocean beach when the surf is "up" (large amplitude waves). These are usually generated by turbulent winds in storms in the distant ocean, 1000 km or farther from shore. The shortest wavelengths present should be those for which the damping length, $C\tau_*$ is about 1000 km; shorter wavelengths than that will have been dissipated before reaching shore. Using the turbulent viscosity $\nu \sim 0.03\,\mathrm{m^2\,s^{-1}}$ that we deduced from the observed thicknesses of wind-driven Ekman layers in the ocean (Ex. 14.21), compute this shortest wavelength for the large amplitude waves, and compare with the wavelengths you have observed at an ocean beach. You should get pretty good agreement, thanks to a weak sensitivity of the wavelength on the rather uncertain turbulent viscosity.

(c) Make similar comparisons of theory and observation for (i) the choppy, short wavelength ocean waves that one sees when (and only when) a local wind is blowing, and (ii) waves on a small lake.

Exercise 16.3 *Example: Shallow-Water Waves with Variable Depth; Tsunamis*[3]

Consider small-amplitude (linear) shallow-water waves in which the height of the bottom boundary varies, so the unperturbed water's depth is variable: $h_o = h_o(x, y)$.

(a) From the theory of non-linear shallow-water waves with variable depth, in Box 16.3, show that the wave equation for the perturbation $\xi(x, y, t)$ of the water's height takes the form

$$\frac{\partial^2 \xi}{\partial t^2} - {}^{(2)}\boldsymbol{\nabla} \cdot (gh_o{}^{(2)}\boldsymbol{\nabla}\xi) = 0 . \tag{16.12}$$

Here ${}^{(2)}\boldsymbol{\nabla}$ is the 2-dimensional gradient operator that acts in the horizontal (x, y) plane. Note that gh_o is the square of the wave's propagation speed C^2 (phase speed and group speed), so this equation takes the form (7.17) that we studied in the geometric optics approximation in Sec. 7.3.1.

---

[3]Exercise courtesy David Stevenson.

(b) Describe what happens to the direction of propagation of a wave as the depth h_o of the water varies (either as a set of discrete jumps in h_o or as a slowly varying h_o). As a specific example, how must the propagation direction change as waves approach a beach (but when they are sufficiently far out from the beach that nonlinearities have not yet caused them to begin to break). Compare with your own observations at a beach.

(c) Tsunamis are gravity waves with enormous wavelengths, ~ 100 km or so, that propagate on the deep ocean. Since the ocean depth is typically $h_o \sim 4$ km, tsunamis are governed by the shallow-water wave equation (16.12). What would you have to do to the ocean floor to create a lens that would focus a tsunami, generated by an earthquake near Japan, so that it destroys Los Angeles? For simulations of tsunami propagation, see, e.g., `http://bullard.esc.cam.ac.uk/~taylor/Tsunami.html` .

(d) The height of a tsunami, when it is in the ocean with depth $h_o \sim 4$ km, is only ~ 1 meter or less. Use the geometric-optics approximation (Sec. 7.3) to show that the tsunami's wavelength decreases as $\lambda \propto \sqrt{h_o}$ and its amplitude increases as $\max(\xi) \propto 1/h_o^{1/4}$ as the tsunami nears land and the water's depth h_o decreases.

(e) How high, $\max(\xi)$, does the tsunami get when nonlinearities become strongly important? (Assume a height of 1 m in the deep ocean.) How does this compare with the heights of historically disastrous tsunamis when they hit land? From your answer you should conclude that the nonlinearities must play a major role in raising the height. Equations (1) in Box 16.3 are used by geophysicists to analyze this nonlinear growth of the tsunami height. If the wave breaks, then these equations fail, and ideas developed (in rudimentary form) in Ex. 17.7 must be used.

****

16.2.3   Capillary Waves and Surface Tension

When the wavelength is very short (so k is very large), we must include the effects of *surface tension* on the surface boundary condition. Surface tension can be treated as an isotropic force per unit length, γ, that lies in the surface and is unaffected by changes in the shape or size of the surface; see Box 16.4. In the case of a gravity wave traveling in the x direction, this tension produces on the fluid's surface a net downward force per unit area $-\gamma d^2\xi/dx^2 = \gamma k^2 \xi$, where k is the horizontal wave number. [This downward force is like that on a curved violin string; cf. Eq. (12.26) and associated discussion.] This additional force must be included in Eq. (16.5) as an augmentation of ρg. Correspondingly, the effect of surface tension on a mode with wave number k is simply to change the true acceleration of gravity to an *effective acceleration of gravity*

$$g \to g + \frac{\gamma k^2}{\rho} \ . \tag{16.13}$$

Box 16.4
Surface Tension

In a water molecule, the two hydrogen atoms stick out from the larger oxygen atom somewhat like Micky Mouse's ears, with an H-O-H angle of 105 degrees. This asymmetry of the molecule gives rise to a large electric dipole moment. In the interior of a body of water, the dipole moments are oriented rather randomly, but near the water's surface they tend to be parallel to the surface and bond with each other so as to create *surface tension* — a macroscopically isotropic, two-dimensional tension force (force per unit length) γ that is confined to the water's surface.

(a)

(b)
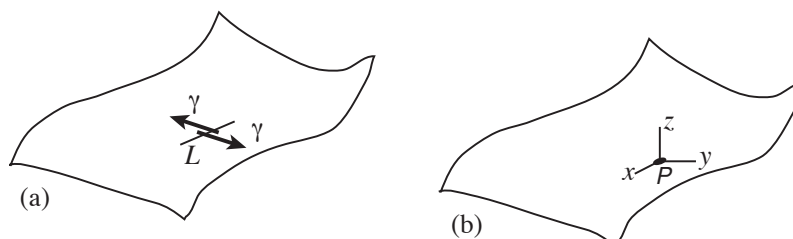
More specifically, consider a line L in the water's surface, with unit length [drawing (a) above]. The surface water on one side of L exerts a tension (pulling) force on the surface water on the other side. The magnitude of this force is γ and it is orthogonal to the line L regardless of L's orientation. This is analogous to an isotropic pressure P in three dimensions, which acts orthogonally across any unit area.

Choose a point $\mathcal{P}$ in the water's surface and introduce local Cartesian coordinates there with x and y lying in the surface and z orthogonal to it [drawing (b) above]. In this coordinate system, the 2-dimensional stress tensor associated with surface tension has components $^{(2)}T_{xx} = {}^{(2)}T_{yy} = -\gamma$, analogous to the 3-dimensional stress tensor for an isotropic pressure, $T_{xx} = T_{yy} = T_{zz} = P$. We can also use a 3-dimensional stress tensor to describe the surface tension: $T_{xx} = T_{yy} = -\gamma\delta(z)$; all other $T_{jk} = 0$. If we integrate this 3-dimensional stress tensor through the water's surface, we obtain the 2-dimensional stress tensor: $\int T_{jk}dz = {}^{(2)}T_{jk}$; i.e., $\int T_{xx}dz = \int T_{yy}dz = -\gamma$. The 2-dimensional metric of the surface is $^{(2)}\mathbf{g} = \mathbf{g} - \mathbf{e}_z \otimes \mathbf{e}_z$; in terms of this 2-dimensional metric, the surface tension's 3-dimensional stress tensor is $\mathbf{T} = -\gamma\delta(z)^{(2)}\mathbf{g}$.

Water is not the only fluid that exhibits surface tension; all fluids do so, at the interfaces between themselves and other substances. For a thin film, e.g. a soap bubble, there are two interfaces (the top face and the bottom face of the film), so if we ignore the film's thickness, its stress tensor is twice as large as for a single surface, $\mathbf{T} = -2\gamma\delta(z)^{(2)}\mathbf{g}$.

The hotter the fluid, the more randomly are oriented its surface molecules and hence the smaller the fluid's surface tension γ. For water, γ varies from 75.6 dyne/cm at $T = 0$ C, to 72.0 dyne/cm at $T = 25$ C, to 58.9 dyne/cm at $T = 100$ C.

In Exs. 16.4–16.6 we explore some applications of surface tension. In Sec. 16.2.3 and Exs. 16.7 and 16.8, we explore the influence of surface tension on water waves. In Ex. 5.14, we explore the statistical thermodynamics of surface tension and its role in the nucleation of water droplets in clouds and fog.

The remainder of the derivation of the dispersion relation for deep gravity waves carries over unchanged, and the dispersion relation becomes

$$\omega^2 = gk + \frac{\gamma k^3}{\rho} \qquad (16.14)$$

[cf. Eqs. (16.9) and (16.13)]. When the second term dominates, the waves are sometimes called *capillary waves*. In Exs. 16.7 and 16.8 we explore some aspects of capillary waves. In Exs. 16.4–16.6 we explore some other aspects of surface tension.

****

EXERCISES

Exercise 16.4 *Problem: Maximum size of a water droplet*
What is the maximum size of water droplets that can form by water very slowly dripping out of a syringe? and out of a water faucet (whose opening is far larger than that of a syringe)?

Exercise 16.5 *Problem: Force Balance for an Interface Between Two Fluids*
Consider a point $\mathcal{P}$ in the curved interface between two fluids. Introduce Cartesian coordinates at $\mathcal{P}$ with x and y parallel to the interface and z orthogonal [as in diagram (b) of Box 16.4], and orient the x and y axes along the directions of the interface's "principal curvatures", so the local equation for the interface is

$$z = \frac{x^2}{2R_1} + \frac{y^2}{2R_2} \; . \qquad (16.15)$$

Here R_1 and R_2 are the surface's "principal radii of curvature" at $\mathcal{P}$; note that each of them can be positive or negative, depending on whether the surface bends up or down along their directions. Show that, in equilibrium, stress balance $\boldsymbol{\nabla} \cdot \mathbf{T} = 0$ for the surface implies that the pressure difference across the surface is

$$\Delta P = \gamma \left(\frac{1}{R_1} + \frac{1}{R_2} \right), \qquad (16.16)$$

where γ is the surface tension.

Exercise 16.6 *Challenge: Minimum Area of Soap Film*
For a soap film that is attached to a bent wire (e.g. to the circular wire that a child uses to blow a bubble), the air pressure on the film's two sides is the same. Therefore, Eq. (16.16) (with γ replaced by 2γ since the film has two faces) tells us that at every point of the film, its two principal radii of curvature must be equal and opposite, $R_1 = -R_2$. It is an interesting excercise in differential geometry to show that this means that the soap film's surface area is an extremum with respect to variations of the film's shape, holding its boundary on the wire fixed. If you know enough differential geometry, prove this extremal-area property of soap films, and then show that, in order for the film's shape to be stable, its extremal area must actually be a minimum.

Exercise 16.7 *Problem: Capillary Waves*
Consider deep-water gravity waves of short enough wavelength that surface tension must be included, so the dispersion relation is Eq. (16.14). Show that there is a minimum value of the group velocity and find its value together with the wavelength of the associated wave. Evaluate these for water ($\gamma \sim 70$ dyne cm^{-1}). Try performing a crude experiment to verify this phenomenon.

Exercise 16.8 *Example: Boat Waves*
A toy boat moves with uniform velocity **u** across a deep pond (Fig. 16.2). Consider the wave pattern (time-independent in the boat's frame) produced on the water's surface at distances large compared to the boat's size. Both gravity waves and surface-tension or *capillary* waves are excited. Show that capillary waves are found both ahead of and behind the boat, and gravity waves, solely inside a trailing wedge. More specifically:

(a) In the rest frame of the water, the waves' dispersion relation is Eq. (16.14). Change notation so ω is the waves' angular velocity as seen in the boat's frame and ω_o in the water's frame, so the dispersion relation is $\omega_o^2 = gk + (\gamma/\rho)k^3$. Use the doppler shift (i.e. the transformation between frames) to derive the boat-frame dispersion relation $\omega(k)$.

(b) The boat radiates a spectrum of waves in all directions. However, only those with vanishing frequency in the boat's frame, $\omega = 0$, contribute to the time-independent ("stationary") pattern. As seen in the water's frame and analyzed in the geometric optics approximation of Chap. 7, these waves are generated by the boat (at points along its horizontal dash-dot trajectory in Fig. 16.2) and travel outward with the group velocity $\mathbf{V}_{go}$. Regard Fig. 16.2 as a snapshot of the boat and water at a particular moment of time. Consider a wave that was generated at an earlier time, when the boat was at location $\mathcal{P}$, and that traveled outward from there with speed V_{go} at an angle ϕ to the boat's direction of motion. (You may restrict yourself to $0 \le \phi \le \pi/2$.) Identify
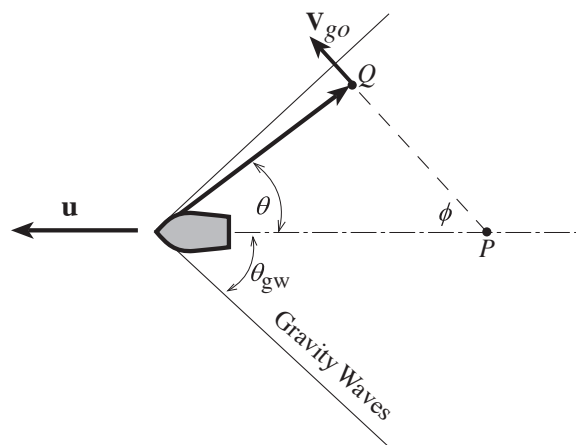

Fig. 16.2: Capillary and gravity waves excited by a small boat (Ex. 16.8).

the point $\mathcal{Q}$ that this wave has reached, at the time of the snapshot, by the angle θ shown in the figure. Show that θ is given by

$$\tan\theta = \frac{V_{go}(k)\sin\phi}{u - V_{go}(k)\cos\phi} \; , \tag{16.17a}$$

where k is determined by the dispersion relation $\omega_0(k)$ together with the "vanishing ω" condition

$$\omega_0(k,\phi) = uk\cos\phi \; . \tag{16.17b}$$

(c) Specialize to capillary waves $[k \gg \sqrt{g\rho/\gamma}]$. Show that

$$\tan\theta = \frac{3\tan\phi}{2\tan^2\phi - 1} \; . \tag{16.18}$$

Demonstrate that the capillary wave pattern is present for all values of θ (including in front of the boat, $\pi/2 < \theta < \pi$, and behind it, $0 \le \theta \le \pi/2$).

(d) Next, specialize to gravity waves and show that

$$\tan\theta = \frac{\tan\phi}{2\tan^2\phi + 1} \; . \tag{16.19}$$

Demonstrate that the gravity-wave pattern is confined to a trailing wedge with angles $\theta < \theta_{\rm gw} = \sin^{-1}(1/3) = 19.47°$; cf. Fig. 16.2. You might try to reproduce these results experimentally.

<p style="text-align:center">***************************</p>

16.2.4 Helioseismology

The sun provides an excellent example of the excitation of small amplitude waves in a fluid body. In the 1960s, Robert Leighton and colleagues discovered that the surface of the sun oscillates vertically with a period of roughly five minutes and a speed of ~ 1 km s^{-1}. This was thought to be an incoherent surface phenomenon until it was shown that the observed variation was, in fact, the superposition of thousands of highly coherent wave modes excited within the sun's interior — normal modes of the sun. Present day techniques allow surface velocity amplitudes as small as 2 mm s^{-1} to be measured, and phase coherence for intervals as long as a year has been observed. Studying the frequency spectrum and its variation provides a unique probe of the sun's interior structure, just as the measurement of conventional seismic waves, as described in Sec.12.4, probes the earth's interior.

   The description of the sun's normal modes requires some modification of our treatment of gravity waves. We shall eschew details and just outline the principles—which are rather similar to those for normal modes of a homogeneous elastic sphere (Sec. 12.4.4 and Ex. 12.12).

First, the sun is (very nearly) spherical. We therefore work in spherical polar coordinates rather than Cartesian coordinates. Second, the sun is made of hot gas and it is no longer a good approximation to assume that the fluid is always incompressible. We must therefore replace the equation $\nabla \cdot \mathbf{v} = 0$ with the full equation of continuity (mass conservation) together with the equation of energy conservation which governs the relationship between the perturbations of density and pressure. Third, the sun is not uniform. The pressure and density in the unperturbed gas vary with radius in a known manner and must be included. Fourth, the sun has a finite surface area. Instead of assuming that there will be a continuous spectrum of waves, we must now anticipate that the boundary conditions will lead to a discrete spectrum of normal modes. Allowing for these complications, it is possible to derive a differential equation for the perturbations to replace Eq. (16.7). It turns out that a convenient dependent variable (replacing the velocity potential ψ) is the pressure perturbation. The boundary conditions are that the displacement vanish at the center of the sun and the pressure perturbation vanish at the surface.

At this point the problem is reminiscent of the famous solution for the eigenfunctions of the Schrödinger equation for a hydrogen atom in terms of associated Laguerre polynomials. The wave frequencies of the sun's normal modes are given by the eigenvalues of the differential equation. The corresponding eigenfunctions can be classified using three quantum numbers, n, l, m, where n counts the number of radial nodes in the eigenfunction and the angular variation of the pressure perturbation is proportional to the spherical harmonic $Y_l^m(\theta, \phi)$. If the sun were precisely spherical, the modes with the same n and l but different m would be degenerate, just as is the case with an atom when there is no preferred direction in space. However, the sun rotates with a latitude-dependent period in the range $\sim 25 - 30$ days and this breaks the degeneracy just as an applied magnetic field in an atom breaks the degeneracy of the atom's states (the Zeeman effect). From the observed splitting of the solar-mode spectrum, it is possible to learn about the distribution of rotational angular momentum inside the sun.

When this problem is solved in detail, it turns out that there are two general classes of modes. One class is similar to gravity waves, in the sense that the forces which drive the gas's motions are produced primarily by gravity (either directly, or indirectly via the weight of overlying material producing pressure that pushes on the gas.) These are called *g modes*. In the second class (known as *p* and *f modes*), the pressure forces arise mainly from the compression of the fluid just like in sound waves (which we shall study in Sec. 16.5 below). Now, it turns out that the *g* modes have large amplitudes in the middle of the sun, whereas the *p* and *f* modes are dominant in the outer layers (cf. Fig. 16.3b). The reasons for this are relatively easy to understand and introduce ideas to which we shall return:

The sun is a hot body, much hotter at its center ($T \sim 1.5 \times 10^7$ K) than on its surface ($T \sim 6000$ K). The sound speed C is therefore much greater in its interior and so p and f modes of a given frequency ω can carry their energy flux $\sim \rho \xi^2 \omega^2 C$ (Sec.16.5) with much smaller amplitudes ξ than near the surface. Therefore the p- and f-mode amplitudes are much smaller in the center of the sun than near the surface.

The g-modes are controlled by different physics and thus behave differently: The outer ~ 30 percent (by radius) of the sun is *convective* (cf. Chap. 18) because the diffusion of heat is inadequate to carry the huge amount of nuclear energy being generated in the solar core.
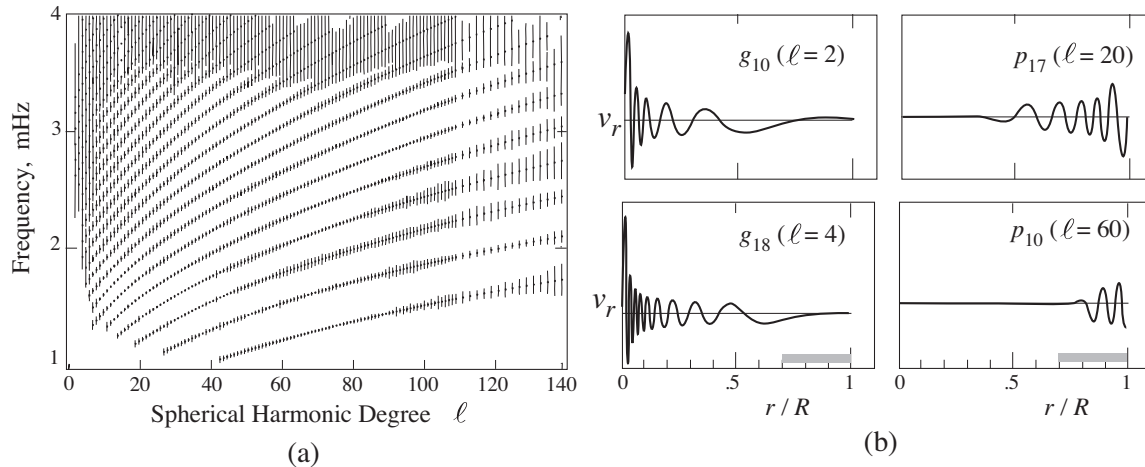
Fig. 16.3: (a) Measured frequency spectrum for solar p-modes with different values of the quantum numbers n, l. The error bars are magnified by a factor 1000. Frequencies for modes with $n > 30$ and $l > 1000$ have been measured. (b) Sample eigenfunctions for g and p modes labeled by n (subscripts) and l (parentheses). The ordinate is the radial velocity and the abscissa is fractional radial distance from the sun's center to its surface. The solar convection zone is the shaded region at the bottom. (Adapted from Libbrecht and Woodard 1991.)

The convection produces an equilibrium variation of pressure and density with radius that are just such as to keep the sun almost neutrally stable, so that regions that are slightly hotter (cooler) than their surroundings will rise (sink) in the solar gravitational field. Therefore there cannot be much of a mechanical restoring force which would cause these regions to oscillate about their average positions, and so the g modes (which are influenced almost solely by gravity) have little restoring force and thus are *evanescent* in the convection zone, and so their amplitudes decay quickly with increasing radius there.

We should therefore expect only p and f modes to be seen in the surface motions and this is, indeed the case. Furthermore, we should not expect the properties of these modes to be very sensitive to the physical conditions in the core. A more detailed analysis bears this out.

16.3 Nonlinear Shallow-Water Waves and Solitons

In recent decades, *solitons* or solitary waves have been studied intensively in many different areas of physics. However, fluid dynamicists became familiar with them in the nineteenth century. In an oft-quoted passage, John Scott-Russell (1844) described how he was riding along a narrow canal and watched a boat stop abruptly. This deceleration launched a single smooth pulse of water which he followed on horseback for one or two miles, observing it "rolling on a rate of some eight or nine miles an hour, preserving its original figure some thirty feet long and a foot to a foot and a half in height". This was a soliton – a one dimensional, nonlinear wave with fixed profile traveling with constant speed. Solitons can be observed fairly readily when gravity waves are produced in shallow, narrow channels. We

shall use the particular example of a shallow, nonlinear gravity wave to illustrate solitons in general.

16.3.1   Korteweg-de Vries (KdV) Equation

The key to a soliton's behavior is a robust balance between the effects of dispersion and the effects of nonlinearity. When one grafts these two effects onto the wave equation for shallow water waves, then at leading order in the strengths of the dispersion and nonlinearity one gets the *Korteweg-de Vries* (KdV) equation for solitons. Since a completely rigorous derivation of the KdV equation is quite lengthy, we shall content ourselves with a somewhat heuristic derivation that is based on this grafting process, and is designed to emphasize the equation's physical content.

   We choose as the dependent variable in our wave equation the height ξ of the water's surface above its quiescent position, and we confine ourselves to a plane wave that propagates in the horizontal x direction so $\xi = \xi(x, t)$.

   In the limit of very weak waves, $\xi(x, t)$ is governed by the shallow-water dispersion relation $\omega = \sqrt{gh_o}\, k$, where h_o is the depth of the quiescent water. This dispersion relation implies that $\xi(x, t)$ must satisfy the following elementary wave equation [cf. Eq. (16.12)]:

$$0 = \frac{\partial^2 \xi}{\partial t^2} - gh_o \frac{\partial^2 \xi}{\partial x^2} = \left(\frac{\partial}{\partial t} - \sqrt{gh_o} \frac{\partial}{\partial x} \right) \left(\frac{\partial}{\partial t} + \sqrt{gh_o} \frac{\partial}{\partial x} \right) \xi \; . \tag{16.20}$$

In the second expression, we have factored the wave operator into two pieces, one that governs waves propagating rightward, and the other leftward. To simplify our derivation and the final wave equation, we shall confine ourselves to rightward propagating waves, and correspondingly we can simply remove the left-propagation operator, obtaining

$$\frac{\partial \xi}{\partial t} + \sqrt{gh_o} \frac{\partial \xi}{\partial x} = 0 \; . \tag{16.21}$$

(Leftward propagating waves are described by this same equation with a change of sign.)

   We now graft the effects of dispersion onto this rightward wave equation. The dispersion relation, including the effects of dispersion at leading order, is $\omega = \sqrt{gh_o}\, k(1 - \frac{1}{6} k^2 h_o^2)$ [Eq. (16.11)]. Now, this dispersion relation ought to be derivable by assuming a variation $\xi \propto \exp[i(kx - \omega t)]$ and substituting into a generalization of Eq. (16.21) with corrections that take account of the finite depth of the channel. We will take a short cut and reverse this process to obtain the generalization of Eq. (16.21) from the dispersion relation. The result is

$$\frac{\partial \xi}{\partial t} + \sqrt{gh_o} \frac{\partial \xi}{\partial x} = -\frac{1}{6} \sqrt{gh_o} \, h_o^2 \frac{\partial^3 \xi}{\partial x^3} \; , \tag{16.22}$$

as a simple calculation confirms. This is the "linearized KdV equation". It incorporates weak dispersion associated with the finite depth of the channel but is still a linear equation, only useful for small-amplitude waves.

   Now let us set aside the dispersive correction and tackle the nonlinearity using the equations derived in Box 16.3. Denoting the depth of the disturbed water by $h = h_o + \xi$, the

nonlinear law of mass conservation [Eq. (1a) of Box 16.3] becomes

$$\frac{\partial h}{\partial t} + \frac{\partial (hv)}{\partial x} = 0 \ , \tag{16.23a}$$

and the Navier Stokes equation [Eq. (1b) of Box 16.3] becomes

$$\frac{\partial v}{\partial t} + v\frac{\partial v}{\partial x} + g\frac{\partial h}{\partial x} = 0 \ . \tag{16.23b}$$

Here we have specialized the equations in Box 16.3 to a one-dimensional wave in the channel and to a constant depth h_o of the channel's undisturbed water. Equations (16.23a) and (16.23b) can be combined to obtain

$$\frac{\partial \left(v - 2\sqrt{gh}\right)}{\partial t} + \left(v - \sqrt{gh}\right)\frac{\partial \left(v - 2\sqrt{gh}\right)}{\partial x} = 0 \ . \tag{16.23c}$$

This equation shows that the quantity $v - 2\sqrt{gh}$ is constant along characteristics that propagate with speed $v - \sqrt{gh}$. (This constant quantity is a special case of a *Riemann invariant*, a concept that we shall study in Chap. 17.) When, as we shall require below, the nonlinearites are modest so h does not differ greatly from h_o, these characteristics propagate leftward, which implies that for rightward propagating waves they begin at early times in undisturbed fluid where $v = 0$ and $h = h_o$. Therefore, the constant value of $v - 2\sqrt{gh}$ is $-2\sqrt{gh_o}$, and correspondingly in regions of disturbed fluid

$$v = 2\left(\sqrt{gh} - \sqrt{gh_o}\right) \ . \tag{16.24}$$

Substituting this into Eq. (16.23a), we obtain

$$\frac{\partial h}{\partial t} + \left(3\sqrt{gh} - 2\sqrt{gh_o}\right)\frac{\partial h}{\partial x} = 0 \ . \tag{16.25}$$

We next substitute $\xi = h - h_o$ and expand to second order in ξ to obtain the final form of our wave equation with nonlinearities but no dispersion:

$$\frac{\partial \xi}{\partial t} + \sqrt{gh_o}\frac{\partial \xi}{\partial x} = -\frac{3\xi}{2}\sqrt{\frac{g}{h_o}}\frac{\partial \xi}{\partial x} \ , \tag{16.26}$$

where the term on the right hand side is the nonlinear correction.

We now have separate dispersive corrections (16.22) and nonlinear corrections (16.26) to the rightward wave equation (16.21). Combining the two corrections into a single equation, we obtain

$$\frac{\partial \xi}{\partial t} + \sqrt{gh_o}\left[\left(1 + \frac{3\xi}{2h_o}\right)\frac{\partial \xi}{\partial x} + \frac{h_o^2}{6}\frac{\partial^3 \xi}{\partial x^3}\right] = 0 \ . \tag{16.27}$$

Finally, we substitute

$$\boxed{\chi \equiv x - \sqrt{gh_o}\,t} \tag{16.28}$$

to transform into a frame moving rightward with the speed of small-amplitude gravity waves. The result is the full *Korteweg-deVries* or KdV equation:

$$\boxed{\frac{\partial \xi}{\partial t} + \frac{3}{2}\sqrt{\frac{g}{h_o}}\left(\xi\frac{\partial \xi}{\partial \chi} + \frac{1}{9}h_o^3\frac{\partial^3 \xi}{\partial \chi^3}\right) = 0} \ . \tag{16.29}$$

16.3.2 Physical Effects in the KdV Equation

Before exploring solutions to the KdV equation (16.29), let us consider the physical effects of its nonlinear and dispersive terms. The second (nonlinear) term $\frac{3}{2}\sqrt{g/h_o}\,\xi\partial\xi/\partial\chi$ derives from the nonlinearity in the $(\mathbf{v}\cdot\nabla)\mathbf{v}$ term of the Navier-Stokes equation. The effect of this nonlinearity is to steepen the leading edge of a wave profile and flatten the trailing edge (Fig. 16.4.) Another way to understand the effect of this term is to regard it as a nonlinear coupling of linear waves. Since it is nonlinear in the wave amplitude, it can couple together waves with different wave numbers k. For example, if we have a purely sinusoidal wave $\propto \exp(ikx)$, then this nonlinearity will lead to the growth of a first harmonic $\propto \exp(2ikx)$. Similarly, when two linear waves with spatial frequencies k, k' are superposed, this term will describe the production of new waves at the sum and difference spatial frequencies. We have already met such wave-wave coupling in our study of nonlinear optics (Chap. 10), and in the route to turbulence for rotating Couette flow (Fig. 15.16), and we shall meet it again in nonlinear plasma physics (Chap. 23).

The third term in (16.29), $\frac{1}{6}\sqrt{g/h_o}\,h_o^3\,\partial^3\xi/\partial\chi^3$, is linear and is responsible for a weak dispersion of the wave. The higher-frequency Fourier components travel with slower phase velocities than lower-frequency components. This has two effects. One is an overall spreading of a wave in a manner qualitatively familiar from elementary quantum mechanics; cf. Ex. 7.2. For example, in a Gaussian wave packet with width Δx, the range of wave numbers k contributing significantly to the profile is $\Delta k \sim 1/\Delta x$. The spread in the group velocity is then $\sim \Delta k\,\partial^2\omega/\partial k^2 \sim (gh_o)^{1/2}h_o^2\,k\Delta k$ [cf. Eq. (16.11)]. The wave packet will then double in size in a time

$$t_{spread} \sim \frac{\Delta x}{\Delta v_g} \sim \left(\frac{\Delta x}{h_o}\right)^2 \frac{1}{k\sqrt{gh_o}}\,. \tag{16.30}$$

The second effect is that since the high-frequency components travel somewhat slower than the low-frequency components, there will be a tendency for the profile to become asymmetric with the leading edge less steep than the trailing edge.

Given the opposite effects of these two corrections (nonlinearity makes the wave's leading edge steeper; dispersion reduces its steepness), it should not be too surprising in hindsight that it is possible to find solutions to the KdV equation in which nonlinearity balances
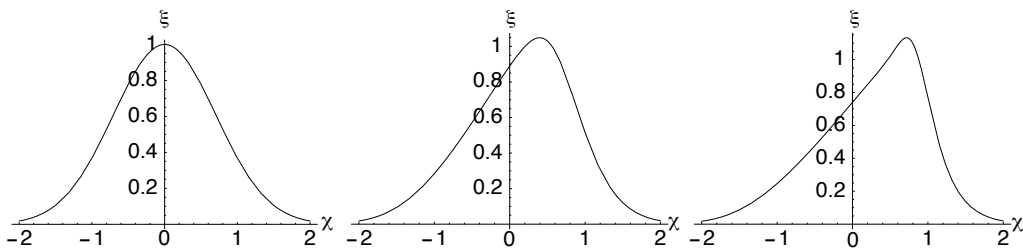

Fig. 16.4: Steepening of a Gaussian wave profile by the nonlinear term in the KdV equation. The increase of wave speed with amplitude causes the leading part of the profile to steepen with time and the trailing part to flatten. In the full KdV equation, this effect can be balanced by the effect of dispersion, which causes the high-frequency Fourier components in the wave to travel slightly slower than the low-frequency components. This allows stable solitons to form.
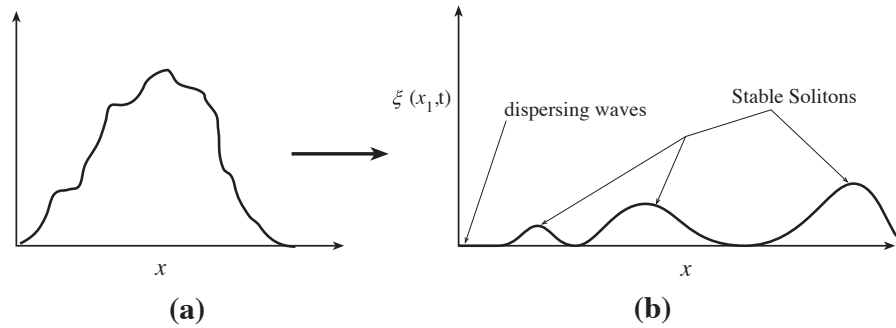
Fig. 16.5: Production of stable solitons out of an irregular initial wave profile.

dispersion, so there is no change of shape as the wave propagates and no spreading. What is quite surprising, though, is that these solutions, called *solitons*, are very robust and arise naturally out of random initial data. That is to say, if we solve an initial value problem numerically starting with several peaks of random shape and size, then although much of the wave will spread and disappear due to dispersion, we will typically be left with several smooth soliton solutions, as in Fig. 16.5.

16.3.3 Single-Soliton Solution

We can discard some unnecessary algebraic luggage in the KdV equation (16.29) by transforming both independent variables using the substitutions

$$\zeta = \frac{\xi}{h_o} \ , \quad \eta = \frac{3\chi}{h_o} = \frac{3(x - \sqrt{gh_o}\,t)}{h_o} \ , \quad \tau = \frac{9}{2}\sqrt{\frac{g}{h_o}}\,t \ . \tag{16.31}$$

The KdV equation then becomes

$$\frac{\partial \zeta}{\partial \tau} + \zeta \frac{\partial \zeta}{\partial \eta} + \frac{\partial^3 \zeta}{\partial \eta^3} = 0 \ . \tag{16.32}$$

There are well understood mathematical techniques[4] for solving equations like the KdV equation. However, we shall just quote solutions and explore their properties. The simplest solution to the dimensionless KdV equation (16.32) is

$$\zeta = \zeta_0 \, \mathrm{sech}^2\left[\left(\frac{\zeta_0}{12}\right)^{1/2}\left(\eta - \frac{1}{3}\zeta_0\tau\right)\right] \ . \tag{16.33}$$

This solution, depicted in Fig. 16.6, describes a one-parameter family of stable solitons. For each such soliton (each ζ_0), the soliton maintains its shape while propagating at speed

---

[4]See, for example, Whitham (1974).

$\chi_{1/2} = (4h_\text{o}{}^3/3\xi_\text{o})^{1/2}$

ξ_0

$(gh_\text{o})^{1/2}\left[1 + \left(\frac{\xi_\text{o}}{2h_\text{o}}\right)\right]$
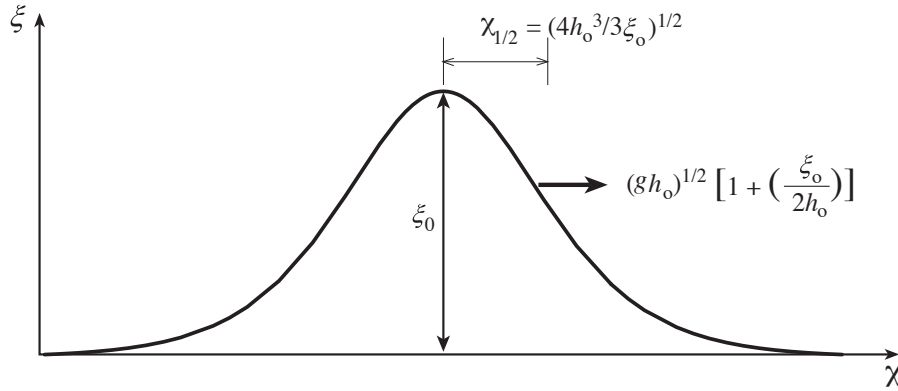
Fig. 16.6: Profile of the single-soliton solution (16.33), (16.31) of the KdV equation. The width $\chi_{1/2}$ is inversely proportional to the square root of the peak height ξ_o.

$d\eta/d\tau = \zeta_0/3$ relative to a weak wave. By transforming to the rest frame of the unperturbed water using Eqs. (16.31) and (16.28), we find for the soliton's speed there:

$$\frac{dx}{dt} = \sqrt{gh_o}\left[1 + \left(\frac{\xi_o}{2h_o}\right)\right] \ . \tag{16.34}$$

The first term is the propagation speed of a weak (linear) wave. The second term is the nonlinear correction, proportional to the wave amplitude $\xi_o = h_o\zeta_o$. The half width of the wave may be defined by setting the argument of the hyperbolic secant to unity. It is $\eta_{1/2} = (12/\zeta_o)^{1/2}$, corresponding to

$$x_{1/2} = \chi_{1/2} = \left(\frac{4h_o^3}{3\xi_o}\right)^{1/2} \ . \tag{16.35}$$

The larger the wave amplitude, the narrower its length and the faster it propagates; cf. Fig. 16.6.

Let us return to Scott-Russell's soliton. Converting to SI units, the speed was about 4 m s^{-1} giving an estimate of the depth of the canal as $h_o \sim 1.6$ m. Using the width $x_{1/2} \sim 5$ m, we obtain a peak height $\xi_o \sim 0.25$ m, somewhat smaller than quoted but within the errors allowing for the uncertainty in the definition of the width and an (appropriate) element of hyperbole in the account.

16.3.4 Two-Soliton Solution

One of the most fascinating properties of solitons is the way that two or more waves interact. The expectation, derived from physics experience with weakly coupled normal modes, might be that, if we have two well separated solitons propagating in the same direction with the larger wave chasing the smaller wave, then the larger will eventually catch up with the smaller, and nonlinear interactions between the two waves will essentially destroy both, leaving behind a single, irregular pulse which will spread and decay after the interaction. However, this is not what happens. Instead, the two waves pass through each other unscathed
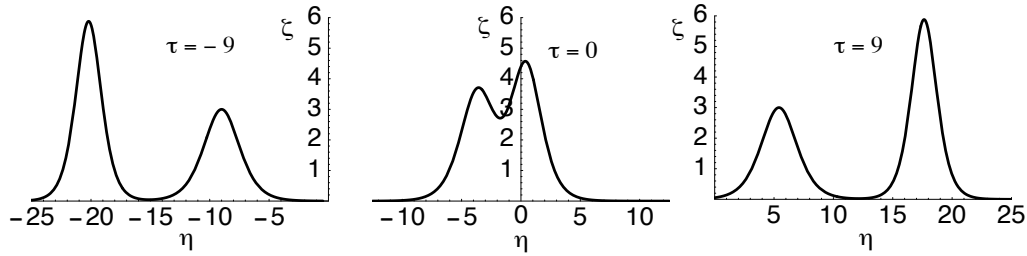
Fig. 16.7: Two-soliton solution to the dimensionless KdV equation (16.32). This solution describes two waves well separated for $\tau \to -\infty$ that coalesce and then separate producing the original two waves in reverse order as $\tau \to +\infty$. The notation is that of Eq. (16.36); the values of the parameters in that equation are $\eta_1 = \eta_2 = 0$ (so the solitons will be merged at time $\eta = 0$), $\alpha_1 = 1$, $\alpha_2 = 1.4$.

and unchanged, except that they emerge from the interaction a bit sooner than they would have had they moved with their original speeds during the interaction. See Fig. 16.7. We shall not pause to explain why the two waves survive unscathed, save to remark that there are topological invariants in the solution which must be preserved. However, we can exhibit one such two-soliton solution analytically:

$$\zeta = \frac{\partial^2}{\partial \eta^2}[12 \ln F(\eta, \tau)] \ ,$$

$$\text{where } F = 1 + f_1 + f_2 + \left(\frac{\alpha_2 - \alpha_1}{\alpha_2 + \alpha_1}\right)^2 f_1 f_2 \ ,$$

$$\text{and } f_i = \exp[-\alpha_i(\eta - \eta_i) + \alpha_i^3 \tau] \ ; \tag{16.36}$$

here α_i and η_i are constants. This solution is depicted in Fig. 16.7.

16.3.5 Solitons in Contemporary Physics

Solitons were re-discovered in the 1960's when they were found in numerical simulations of plasma waves. Their topological properties were soon discovered and general methods to generate solutions were derived. Solitons have been isolated in such different subjects as the propagation of magnetic flux in a Josephson junction, elastic waves in anharmonic crystals, quantum field theory (as *instantons*) and classical general relativity (as solitary, nonlinear gravitational waves). Most classical solitons are solutions to one of a relatively small number of nonlinear ordinary differential equations, including the KdV equation, the *nonlinear Schrödinger equation* which governs solitons in optical fibers (Sec. 10.8.3), *Burgers' equation* and the *sine-Gordon* equation. Unfortunately it has proved difficult to generalize these equations and their soliton solutions to two and three spatial dimensions.

Just like research into chaos (Sec. 15.6), studies of solitons have taught physicists that nonlinearity need not lead to maximal disorder in physical systems, but instead can create surprisingly stable, ordered structures.
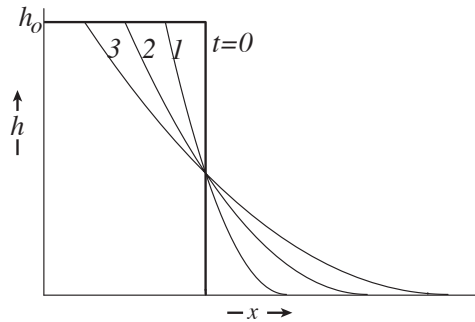
****
EXERCISES

Fig. 16.8: The water's height $h(x,t)$ after a dam breaks.

Exercise 16.9 *Example: Breaking of a Dam*
Consider the flow of water along a horizontal channel of constant width after a dam breaks.
Sometime after the initial transients have died away,[5] the flow may be described by the
nonlinear, unidirectional, shallow-water wave equations (16.23a) and (16.23b):

$$\frac{\partial h}{\partial t} + \frac{\partial(hv)}{\partial x} = 0 \;, \quad \frac{\partial v}{\partial t} + v\frac{\partial v}{\partial x} + g\frac{\partial h}{\partial x} = 0 \;. \tag{16.37}$$

Here h is the height of the flow, v is the horizontal speed of the flow and x is distance along
the channel measured from the location of the dam. Solve for the flow assuming that initially
(at $t = 0$) $h = h_o$ for $x < 0$ and $h = 0$ for $x > 0$ (no water). Your solution should have
the form shown in Fig. 16.8. What is the speed of the front of the water? [*Hints:* Note
that from the parameters of the problem we can construct only one velocity, $\sqrt{gh_o}$ and no
length except h_o. It therefore is a reasonable guess that the solution has the self-similar form
$h = h_o\,\tilde{h}(\xi)$, $v = \sqrt{gh_o}\,\tilde{v}(\xi)$, where $\tilde{h}$ and $\tilde{v}$ are dimensionless functions of the similarity
variable

$$\xi = \frac{x/t}{\sqrt{gh_o}} \;. \tag{16.38}$$

Using this ansatz, convert the partial differential equations (16.37) into a pair of ordinary
differential equations which can be solved so as to satisfy the initial conditions.]

Exercise 16.10 *Derivation: Single-Soliton Solution*
Verify that expression (16.33) does indeed satisfy the dimensionless KdV equation (16.32).

Exercise 16.11 *Derivation: Two-Soliton Solution*

(a) Verify, using symbolic-manipulation computer software (e.g., Maple or Mathematica) that the two-soliton expression (16.36) satisfies the dimensionless KdV equation.
    (Warning: Considerable algebraic travail is required to verify this by hand, directly.)

(b) Verify, analytically, that the two-soliton solution (16.36) has the properties claimed
    in the text: First consider the solution at early times in the spatial region where

---

[5]In the idealized case that the dam is removed instantaneously, there will be no transients and Eqs.
(16.37) will describe the flow from the outset.

$f_1 \sim 1, f_2 \ll 1$. Show that the solution is approximately that of the single soliton described by Eq. (16.33). Demonstrate that the amplitude is $\zeta_{01} = 3\alpha_1^2$ and find the location of its peak. Repeat the exercise for the second wave and for late times.

(c) Use a computer to follow, numerically, the evolution of this two-soliton solution as time η passes (thereby filling in timesteps between those shown in Fig. 16.7).

<div align="center">****************************</div>

16.4 Rossby Waves in a Rotating Fluid

In a nearly rigidly rotating fluid, with the rotational angular velocity $\boldsymbol{\Omega}$ parallel or antiparallel to the acceleration of gravity $\boldsymbol{g} = -g\mathbf{e}_z$, the Coriolis effect observed in the co-rotating reference frame (Sec. 14.5) provides the restoring force for an unusual type of wave motion called "Rossby waves." These waves are seen in the Earth's oceans and atmosphere [with $\boldsymbol{\Omega} =$ (Earth's rotational angular velocity) sin(latitude) $\mathbf{e}_z$; see Box 14.5].

For a simple example, we consider the sea above a sloping seabed; Fig. 16.9. We assume the unperturbed fluid has vanishing velocity $\mathbf{v} = 0$ in the Earth's rotating frame, and we study weak waves in the sea with oscillating velocity $\mathbf{v}$. (Since the fluid is at rest in the equilibrium state about which we are perturbing, we write the perturbed velocity as $\mathbf{v}$ rather than $\delta\mathbf{v}$.) We assume that the wavelengths are long enough that viscosity and surface tension are negligible. We also, in this case, restrict attention to small-amplitude waves so that nonlinear terms can be dropped from our dynamical equations. The perturbed Navier-Stokes equation (14.56a) then becomes (after linearization)

$$\frac{\partial \mathbf{v}}{\partial t} + 2\boldsymbol{\Omega} \times \mathbf{v} = \frac{-\boldsymbol{\nabla}\delta P'}{\rho} \; . \tag{16.39}$$

Here, as in Sec. 14.5, $\delta P'$ is the perturbation in the effective pressure [which includes gravitational and centrifugal effects, $P' = P + \rho\Phi - \frac{1}{2}\rho(\boldsymbol{\Omega} \times \mathbf{x})^2$]. Taking the curl of Eq. (16.39), we obtain for the time derivative of the waves' vorticity

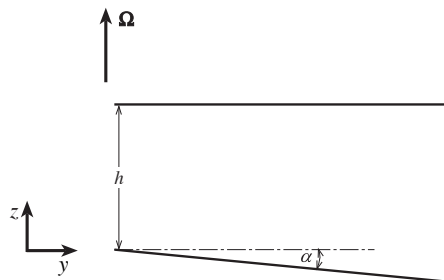$$\frac{\partial \boldsymbol{\omega}}{\partial t} = 2(\boldsymbol{\Omega} \cdot \nabla)\mathbf{v} \; . \tag{16.40}$$

Fig. 16.9: Geometry of ocean for Rossby waves.

We seek a wave mode with angular frequency ω and wave number k, in which the horizontal fluid velocity oscillates in the x direction and (in accord with the Taylor-Proudman theorem, Sec. 14.5.3) is independent of z, so

$$v_x \text{ and } v_y \propto \exp[i(kx - \omega t)] , \quad \frac{\partial v_x}{\partial z} = \frac{\partial v_y}{\partial z} = 0 . \tag{16.41}$$

The only allowed vertical variation is in the vertical velocity v_z, and differentiating $\boldsymbol{\nabla} \cdot \mathbf{v} = 0$ with respect to z, we obtain

$$\frac{\partial^2 v_z}{\partial z^2} = 0 . \tag{16.42}$$

The vertical velocity therefore varies linearly between the surface and the sea floor (Fig. 16.9). Now, one boundary condition is that the vertical velocity must vanish at the sea's surface. The other is that, at the sea floor $z = -h$, we must have $v_z(-h) = -\alpha v_y$, where α is the tangent of the angle of inclination of the sea floor. The solution to Eq. (16.42) satisfying these boundary conditions is

$$v_z = \frac{\alpha z}{h} v_y . \tag{16.43}$$

Taking the vertical component of Eq. (16.40) and evaluating $\omega_z = v_{y,x} - v_{x,y} = ikv_y$, we obtain

$$\omega k v_y = 2\Omega \frac{\partial v_z}{\partial z} = \frac{2\Omega \alpha v_y}{h} . \tag{16.44}$$

The dispersion relation therefore has the quite unusual form $\omega \propto 1/k$:

$$\boxed{\omega k = \frac{2\Omega \alpha}{h}} . \tag{16.45}$$

Rossby waves have interesting properties: They can only propagate in one direction—parallel to the intersection of the sea floor with the horizontal (our $\mathbf{e}_x$ direction). Their phase velocity $\mathbf{V}_{\mathrm{ph}}$ and group velocity $\mathbf{V}_g$ are equal in magnitude but in opposite directions,

$$\mathbf{V}_{\mathrm{ph}} = -\mathbf{V}_g = \frac{2\Omega \alpha}{k^2 h} \mathbf{e}_x . \tag{16.46}$$

If we use $\boldsymbol{\nabla} \cdot \mathbf{v} = 0$, we discover that the two components of horizontal velocity are in quadrature, $v_x = i\alpha v_y/kh$. This means that, when seen from above, the fluid circulates with the opposite sense to the angular velocity Ω.

Rossby waves play an important role in the circulation of the earth's oceans; see, e.g., Chelton and Schlax (1996). A variant of these Rossby waves in air can be seen as undulations in the atmosphere's jet stream, produced when the stream goes over a sloping terrain such as that of the Rocky Mountains. Another variant in neutron stars, called r-modes, generates gravitational waves (ripples of spacetime curvature) that are a promising source for ground-based gravitational-wave detectors such as LIGO.

****
EXERCISES

Exercise 16.12 *Example: Rossby Waves in a Cylndrical Tank with Sloping Bottom*

In the film *Rotating Fluids* by David Fultz (1969), about 20 minutes 40 seconds into the film, an experiment is described in which Rossby waves are excited in a rotating cylindrical tank with inner and outer vertical walls and a sloping bottom. Figure 16.10a is a photograph of the tank from the side, showing its bottom which slopes upward toward the center, and a bump on the bottom which generates the Rossby waves. The tank is filled with water, then set into rotation with an angular velocity Ω; the water is given time to settle down into rigid rotation with the cylinder. Then the cylinder's angular velocity is reduced by a small amount, so the water is rotating at angular velocity $\Delta\Omega \ll \Omega$ relative to the cylinder. As the water passes over the hump on the tank bottom, the hump generates Rossby waves. Those waves are made visible by injecting dye at a fixed radius, through a syringe attached to the tank. Figure 16.10b is a photograph of the dye trace as seen looking down on the tank from above. If there were no Rossby waves present, the trace would be circular. The Rossby waves make it pentagonal. In this exercise you will work out the details of the Rossby waves, explore their physics, and explain the shape of the trace.

Because the slope of the bottom is cylindrical rather than planar, this is somewhat different from the situation in the text (Fig. 16.9). However, we can deduce the details of the waves in this cylindrical case from those for the planar case by geometric-optics considerations (Sec. 7.3), making modest errors because the wavelength of the waves is not all that small compared to the circumference around the tank.

(a) Using geometric optics, show that the rays along which the waves propagate are circles centered on the tank's symmetry axis.

(b) Focus on the ray that is half way between the inner and outer walls of the tank. Let its radius be a and the depth of the water there be h, and the slope angle of the tank floor be α. Introduce quasi-Cartesian coordinates $x = a\phi$, $y = -\varpi$, where $\{\varpi, \phi, z\}$ are cylindrical coordinates. By translating the Cartesian-coordinate waves of the text into quasi-Cartesian coordinates and noting from Fig. 16.10b that five wavelengths must fit into the circumference around the cylinder, show that the velocity field has the form $v_\varpi, v_\phi, v_z \propto e^{i(5\phi+\omega t)}$ and deduce the ratios of the three components of velocity to each other. This solution has nonzero radial velocity at the walls — a warning that edge effects will modify the waves somewhat. This analysis ignores those edge effects.
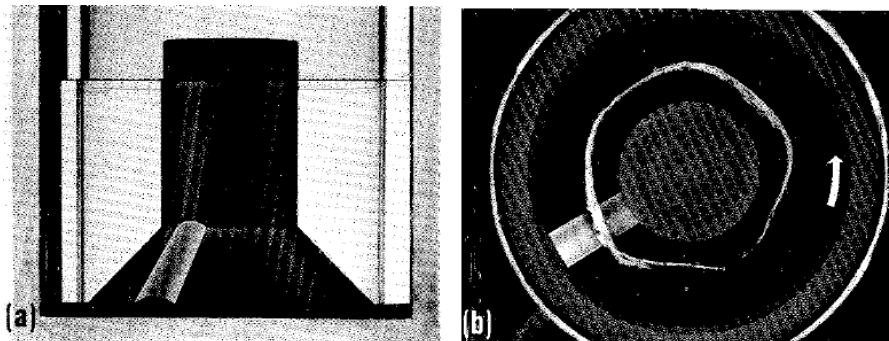

Fig. 16.10: Rossby waves in a rotating cylinder with sloping bottom. From Fultz (1969).

(c) Because the waves are generated by the ridge on the bottom of the tank, the wave pattern must remain at rest relative to that ridge, which means it must rotate relative to the fluid's frame with the angular velocity $d\phi/dt = -\Delta\Omega$. From the waves' dispersion relation deduce $\Delta\Omega/\Omega$, the fractional slowdown of the tank that had to be imposed, in order to generate the observed pentagonal wave.

(d) Compute the displacement field $\delta\mathbf{x}(\varpi, \phi, z, t)$ of a fluid element whose undisplaced location (in the rigidly rotating cylindrical coordinates) is (ϖ, ϕ, z). Explain the pentagonal shape of the movie's dye lines in terms of this displacement field.

(e) Compute the wave's vertical vorticity field ω_z (relative to the rigidly rotating flow), and show that as a fluid element moves, and the vertical vortex line through it shortens or lengths due to the changing water depth, ω_z changes proportionally to the vortex line's length (as it must).

$$****************************$$

16.5 Sound Waves

So far, our discussion of fluid dynamics has mostly been concerned with flows sufficiently slow that the density can be treated as constant. We now introduce the effects of compressibility in the context of sound waves (in a *non*-rotating reference frame). Sound waves are prototypical scalar waves and therefore are simpler in many respects than vector electromagnetic waves and tensor gravitational waves.

Consider a small-amplitude sound wave propagating through a homogeneous, time independent fluid. The wave's oscillations are generally very quick compared to the time for heat to diffuse across a wavelength, so the pressure and density perturbations are adiabatically related:

$$\delta P = C^2 \delta\rho , \tag{16.47}$$

where

$$\boxed{C \equiv \left[\left(\frac{\partial P}{\partial \rho}\right)_s\right]^{1/2}} , \tag{16.48}$$

which will turn out to be the wave's propagation speed — the speed of sound. The perturbation of the fluid velocity (which we denote $\mathbf{v}$ since the unperturbed fluid is static) is related to the pressure perturbation by the linearized Euler equation

$$\frac{\partial \mathbf{v}}{\partial t} = -\frac{\boldsymbol{\nabla}\delta P}{\rho} . \tag{16.49a}$$

A second relation between $\mathbf{v}$ and δP can be obtained by combining the linearized law of mass conservation $\rho \partial \mathbf{v}/\partial t = -\rho \boldsymbol{\nabla}\cdot\mathbf{v}$ with the adiabatic pressure-density relation (16.47):

$$\boldsymbol{\nabla}\cdot\mathbf{v} = -\frac{1}{\rho C^2}\frac{\partial\,\delta P}{\partial t} . \tag{16.49b}$$

By equating the divergence of Eq. (16.49a) to the time derivative of Eq. (16.49b), we obtain a simple, dispersion-free wave equation for the pressure perturbation:

$$\left(\frac{\partial^2}{\partial t^2} - C^2\nabla^2\right)\delta P = 0 \ . \tag{16.50}$$

Thus, as claimed, C is the wave's propagation speed.

For a perfect gas, this adiabatic sound speed is $C = (\gamma P/\rho)^{1/2}$ where γ is the ratio of specific heats (see Ex. 5.4). The sound speed in air at 20°C is 340m s^{-1}. In water under atmospheric conditions, it is about 1.5km s^{-1} (not much different from sound speeds in solids).

Because the vorticity of the unperturbed fluid vanishes and the wave contains no vorticity-producing forces, the wave's vorticity vanishes, $\boldsymbol{\nabla} \times \mathbf{v} = 0$. This permits us to express the wave's velocity perturbation as the gradient of a velocity potential, $\mathbf{v} = \boldsymbol{\nabla}\psi$. Inserting this into the perturbed Euler equation (16.49a) we get the pressure perturbation expressed in terms of ψ:

$$\boxed{\delta P = -\rho\frac{\partial\psi}{\partial t}}, \quad \text{where} \quad \boxed{\mathbf{v} = \boldsymbol{\nabla}\psi} \ . \tag{16.51}$$

The first of these relations guarantees that ψ satisfies the same wave equation as δP:

$$\boxed{\left(\frac{\partial^2}{\partial t^2} - C^2\nabla^2\right)\psi = 0} \ . \tag{16.52}$$

It is sometimes useful to describe the wave by its oscillating pressure δP and sometimes by its oscillating potential ψ.

The general solution of the wave equation (16.52) for plane sound waves propagating in the $\pm x$ directions is

$$\psi = f_1(x - Ct) + f_2(x + Ct) \ , \tag{16.53}$$

where f_1, f_2 are arbitrary functions.

****
EXERCISES

Exercise 16.13 *Problem: Sound Wave in an Inhomogeneous Fluid*
Consider a sound wave propagating through a static, *inhomogeneous* fluid in the absence of gravity. (The inhomogeneity could arise, e.g., from a spatially variable temperature and/or chemical composition.) The unperturbed density and sound speed are functions of location in space, $\rho_o(\mathbf{x})$ and $C(\mathbf{x})$, while the equilibrium pressure P is constant (due to hydrostatic equilibrium) and the equilibrium velocity vanishes.
By repeating the analysis in Eqs. (16.47)–(16.50), show that the wave equation becomes

$$W\frac{\partial^2\delta P}{\partial t^2} - \boldsymbol{\nabla} \cdot (WC^2\boldsymbol{\nabla}\delta P) = 0 \ , \quad \text{where} \quad W = \frac{\rho}{C^2} \ . \tag{16.54}$$

[Hint: It may be helpful to employ the concept of Lagrangian vs. Eulerian perturbations, as described by Eq. (19.41).] Equation (16.54) is an example of the prototypical wave equation

(7.17) that we used in Sec. 7.3.1 to illustrate the geometric-optics formalism. The functional form of W and the placement of W and C^2 (inside vs. outside the derivatives) have *no* influence on the wave's dispersion relation or its rays or phase, in the geometric optics limit, but they *do* influence the propagation of the wave's amplitude. See Sec. 7.3.1.

****

16.5.1 Wave Energy

In Sec. (7.3.1) and Ex. 7.4, we used formal mathematical techniques to derive the energy density U and energy flux $\mathbf{F}$ [Eqs. (7.18)] associated with waves satisfying the prototypical wave equation (16.54). In this section, we shall rederive those U and $\mathbf{F}$ for sound waves using a physical, fluid dynamical analysis. Surprisingly, we will get precisely the same expressions. Because of the formal nature of the arguments leading to Eqs. (7.18), we only had a right to expect the same answer up to some multiplicative constant.

The fluid's energy density is $U = (\frac{1}{2}v^2 + u)\rho$ (Table 13.1 with $\Phi = 0$). The first term is the fluid's kinetic energy density; the second, its internal energy density. The internal energy density can be evaluated by a Taylor expansion in the wave's density perturbation:

$$u\rho = [u\rho] + \left[\left(\frac{\partial(u\rho)}{\partial\rho}\right)_s\right]\delta\rho + \frac{1}{2}\left[\left(\frac{\partial^2(u\rho)}{\partial\rho^2}\right)_s\right]\delta\rho \,, \tag{16.55}$$

where the three coefficients in brackets [] are evaluated at the equilibrium density. The first term in Eq. (16.55) is the energy of the background fluid, so we shall drop it. The second term will average to zero over a wave period, so we shall also drop it. The third term can be simplified using the first law of thermodynamics in the form $du = Tds - Pd(1/\rho)$ (which implies $[\partial(u\rho)/\partial\rho]_s = u + P/\rho$), followed by the definition $h = u + P/\rho$ of enthalpy density, followed by the first law in the form $dh = Tds + dP/\rho$, followed by expression (16.48) for the speed of sound. The result is

$$\left(\frac{\partial^2(u\rho)}{\partial\rho^2}\right)_s = \left(\frac{\partial h}{\partial\rho}\right)_s = \frac{C^2}{\rho} \,. \tag{16.56}$$

Inserting this into the third term of Eq. (16.55) and averaging over a wave period and wavelength, we obtain for the wave energy per unit volume $U = \frac{1}{2}\rho\overline{v^2} + (C^2/2\rho)\overline{\delta\rho^2}$. Using $\mathbf{v} = \boldsymbol{\nabla}\psi$ [the second of Eqs. (16.51)] and $\delta\rho = (\rho/C^2)\partial\psi/\partial t$ [from $\delta\rho = (\partial\rho/\partial P)_s\delta P = \delta P/C^2$ and the first of Eqs. (16.51)], we bring this into the form

$$\boxed{U = \frac{1}{2}\rho\overline{\left[(\boldsymbol{\nabla}\psi)^2 + \frac{1}{C^2}\left(\frac{\partial\psi}{\partial t}\right)^2\right]} = \rho\overline{(\boldsymbol{\nabla}\psi)^2}} \,. \tag{16.57}$$

The second equality can be deduced by multiplying the wave equation (16.52) by ψ and averaging. Thus, *there is equipartition of energy between the kinetic and internal energy terms.*

The energy flux is $\mathbf{F} = (\frac{1}{2}v^2 + h)\rho\mathbf{v}$ (Table 13.1 with $\Phi = 0$). The kinetic energy flux (first term) is third order in the velocity perturbation and therefore vanishes on average. For

a sound wave, the internal energy flux (second term) can be brought into a more useful form by expanding the enthalpy per unit mass:

$$h = [h] + \left[\left(\frac{\partial h}{\partial P}\right)_s\right]\delta P = [h] + \frac{\delta P}{\rho} \ . \tag{16.58}$$

Here we have used the first law of thermodynamics $dh = Tds + (1/\rho)dP$ and adiabaticity of the perturbation, $s =$ constant; and the terms in square brackets are unperturbed quantities. Inserting this into $\mathbf{F} = h\rho\mathbf{v}$ and expressing δP and $\mathbf{v}$ in terms of the velocity potential [Eqs. (16.51)], and averaging over a wave period and wavelength, we obtain for the energy flux $\mathbf{F} = \overline{\rho h \mathbf{v}} = \overline{\delta P \, \mathbf{v}}$, which becomes

$$\mathbf{F} = -\rho\overline{\left(\frac{\partial\psi}{\partial t}\right)\boldsymbol{\nabla}\psi} \ . \tag{16.59}$$

This equation and Eq. (16.57) agree with Eqs. (7.18) [with $W = \rho/C^2$; Eq. ((16.54)], which we derived by formal techniques in Sec. (7.3.1) and Ex. 7.4.

For a locally plane wave with $\psi = \psi_o\cos(\mathbf{k}\cdot\mathbf{x} - \omega t + \varphi)$ (where φ is an arbitrary phase), the energy density (16.57) is $U = \frac{1}{2}\rho\psi_o^2 k^2$, and the energy flux (16.59) is $\mathbf{F} = \frac{1}{2}\rho\psi_o^2\omega\mathbf{k}$. Since, for this dispersion-free wave, the phase and group velocities are both $\mathbf{V} = (\omega/k)\hat{\mathbf{k}} = C\hat{\mathbf{k}}$ (where $\hat{\mathbf{k}} = \mathbf{k}/k$ is the unit vector pointing in the wave-propagation direction), the energy density and flux are related by

$$\boxed{\mathbf{F} = U\mathbf{V} = UC\hat{\mathbf{k}}} \ . \tag{16.60}$$

The energy flux is therefore the product of the energy density and the wave velocity, as it must be [Eq. (7.33), where we see that, if the waves were to have dispersion, it would be the group velocity that appears in this expression].

The energy flux carried by sound is conventionally measured in dB (decibels). The flux in decibels, F_{dB}, is related to the flux F in W m^{-2} by

$$\boxed{F_{\mathrm{dB}} = 120 + 10\log_{10}(F)} \ . \tag{16.61}$$

Sound that is barely audible is about 1 dB. Normal conversation is about 50-60 dB. Jet aircraft, rock concerts and volcanic eruptions can cause exposure to more than 120 dB with consequent damage to the ear.

16.5.2   Sound Generation

So far in this book, we have been concerned with describing how different types of waves propagate. It is also important to understand how they are generated. We now outline some aspects of the theory of sound generation.

The reader should be familiar with the theory of electromagnetic wave emission [e.g., Chap. 9 of Jackson (1999)]. There, one considers a localised region containing moving charges and varying currents. The source can be described as a sum over electric and magnetic multipoles, and each multipole produces a characteristic angular variation of the distant radiation field. The radiation-field amplitude decays inversely with distance from the

source and so the Poynting flux varies with the inverse square of the distance. Integrating over a large sphere gives the total power radiated by the source, broken down into the power radiated by each multipolar component. The ratio of the power in successive multipole pairs [e.g., (magnetic dipole power)/(electric dipole power) $\sim$ (electric quadrupole power)/(electric dipole power)] is typically $\sim (b/\lambda)^2$, where b is the size of the source and $\lambda = 1/k$ is the waves' reduced wavelength. When λ is large compared to b (a situation referred to as *slow motion* since the source's charges then generally move at speeds $\sim (b/\lambda)c$ small compared to the speed of light c), the most powerful radiating multipole is the electric dipole $\mathbf{d}(t)$, unless it happens to be suppressed. The dipole's average emitted power is given by the Larmor formula

$$\mathcal{P} = \frac{\overline{\dddot{\mathbf{d}}^2}}{6\pi\epsilon_0 c^3} , \tag{16.62}$$

where $\ddot{\mathbf{d}}$ is the second time derivative of $\mathbf{d}$, the bar denotes a time average, and c is the speed of light.

This same procedure can be followed when describing sound generation. However, as we are dealing with a scalar wave, sound can have a monopolar source. As an pedagogical example, let us set a small, spherical, elastic ball, surrounded by fluid, into radial oscillation (not necessarily sinusoidal) with oscillation frequencies of order ω, so the emitted waves have reduced wavelengths of order $\lambda = C/\omega$. Let the surface of the ball have radius $a + \xi(t)$, and impose the *slow-motion* and *small-amplitude* conditions that

$$\lambda \gg a \gg |\xi| . \tag{16.63}$$

As the waves will be spherical, the relevant outgoing-wave solution of the wave equation (16.52) is

$$\psi = \frac{f(t - r/C)}{r} , \tag{16.64}$$

where f is a function to be determined. Since the fluid's velocity at the ball's surface must match that of the ball, we have (to first order in $\mathbf{v}$ and ψ)

$$\dot{\xi}\mathbf{e}_r = \mathbf{v}(a, t) = \boldsymbol{\nabla}\psi \simeq -\frac{f(t - a/C)}{a^2}\mathbf{e}_r \simeq -\frac{f(t)}{a^2}\mathbf{e}_r , \tag{16.65}$$

where in the third equality we have used the slow-motion condition $\lambda \gg a$. Solving for $f(t)$ and inserting into Eq. (16.64), we see that

$$\psi(r, t) = -\frac{a^2\dot{\xi}(t - r/C)}{r} . \tag{16.66}$$

It is customary to express the radial velocity perturbation v in terms of an oscillating fluid *monopole moment*

$$\boxed{q = 4\pi\rho a^2 \dot{\xi}} . \tag{16.67}$$

Physically this is the total radial discharge of air mass (i.e. mass per unit time) crossing an imaginary fixed spherical surface of radius slightly larger than that of the oscillating ball.

In terms of q, we have $\dot{\xi}(t) = q(t)/4\pi\rho a^2$. Using this and Eq. (16.66), we compute for the power radiated as sound waves [Eq. (16.59) integrated over a sphere centered on the ball]

$$\boxed{\mathcal{P} = \frac{\overline{\ddot{q}^2}}{4\pi\rho C}}.$$

(16.68)

Note that the power is inversely proportional to the signal speed. This is characteristic of monopolar emission and in contrast to the inverse cube variation for dipolar emission [Eq. (16.62)].

The emission of monopolar waves requires that the volume of the emitting solid body oscillate. When the solid simply oscillates without changing its volume, for example the reed on a musical instrument, dipolar emission will usually dominate. We can think of this as two monopoles of size a in antiphase separated by some displacement $b \sim a$. The velocity potential in the far field is then the sum of two monopolar contributions, which almost cancel. Making a Taylor expansion, we obtain

$$\frac{\psi_{\text{dipole}}}{\psi_{\text{monopole}}} \sim \frac{b}{\lambda} \sim \frac{\omega b}{C} \, ,$$

(16.69)

where ω and λ are the characteristic magnitudes of the angular frequency and reduced wavelength of the waves (which we have not assumed to be precisely sinusoidal).

This reduction of ψ by the slow-motion factor b/λ implies that the dipolar power emission is weaker than the monopolar power by a factor $\sim (b/\lambda)^2$ for similar frequencies and amplitudes of motion—the same factor as for electromagnetic waves (see above). However, to emit dipole radiation, momentum must be given to and removed from the fluid. In other words the fluid must be forced by a solid body. In the absence of such a solid body, the lowest multipole that can be radiated effectively is quadrupolar radiation, which is weaker by yet one more factor of $(b/\lambda)^2$.

These considerations are important for understanding how noise is produced by the intense turbulence created by jet engines, especially close to airports. We expect that the sound emitted by the free turbulence in the wake just behind the engine will be quadrupolar and will be dominated by emission from the largest (and hence fastest) turbulent eddies. [See the discussion of turbulent eddies in Sec. 15.4.4.] Denote by ℓ and v_ℓ the size and turnover speed of these largest eddies. Then the characteristic size of the sound's source will be $a \sim b \sim \ell$, the mass discharge will be $q \sim \rho\ell^2 v_\ell$, the characteristic frequency will be $\omega \sim v_\ell/\ell$, the reduced wavelength of the sound waves will be $\lambda = c/\omega \sim \ell c/v_\ell$, and the slow-motion parameter will be $b/\lambda \sim \omega b/c \sim v_\ell/c$. The quadrupolar power radiated per unit volume [Eq. (16.68) divided by the volume ℓ^3 of an eddy and reduced by $\sim (b/\lambda)^4$] will therefore be

$$\frac{d\mathcal{P}}{d^3 x} \sim \rho\frac{v_\ell^3}{\ell}\left(\frac{v_\ell}{c}\right)^5 \, ,$$

(16.70)

and this power will be concentrated around frequency $\omega \sim v_\ell/\ell$. For air of fixed sound speed and length scale, and for which the largest eddy speed is proportional to some characteristic speed V (e.g. the average speed of the air leaving the engine), *the sound generation increases proportional to the eighth power of the Mach number $M = V/C$.* This is known as Lighthill's law. The implications for the design of jet engines should be obvious.

****

EXERCISES

Exercise 16.14 *Problem: Aerodynamic Sound Generation*
Consider the emission of quadrupolar sound waves by a Kolmogorov spectrum of free turbulence (Sec. 15.4.4). Show that the power radiated per unit frequency interval has a spectrum

$$\mathcal{P}_\omega \propto \omega^{-7/2} \ .$$

Also show that the total power radiated is roughly a fraction M^5 of the power dissipated in the turbulence, where M is the Mach number.

****

16.5.3 $\boxed{\text{T2}}$ Radiation Reaction, Runaway Solutions, and Matched Asymptotic Expansions

Let us return to our idealized example of sound waves produced by a radially oscillating, spherical ball. We shall use this example to illustrate several deep issues in theoretical physics: the *radiation-reaction force* that acts back on a source due to its emission of radiation, a spurious *runaway solution* to the source's equation of motion caused by the radiation-reaction force, and *matched asymptotic expansions*, a mathematical technique for solving field equations when there are two different regions of space in which the equations have rather different behaviors.[6] These issues also arise, in a rather more complicated way, in analyses of the radiation reaction force caused by emission of gravitational waves; see the derivation, by Burke (1971), of results quoted in Sec. 27.5.3.

For our oscillating ball, the two different regions of space that we shall match to each other are the *near zone*, $r \ll \lambda$, and the *wave zone*, $r \gtrsim \lambda$.

We consider, first, the near zone, and we redo, from a new point of view, the analysis of the matching of the near-zone fluid velocity to the ball's surface velocity and the computation of the pressure perturbation. Because the region near the ball is small compared to λ and the fluid speeds are small compared to C, the flow is very nearly incompressible, $\boldsymbol{\nabla}\cdot\mathbf{v} = \nabla^2\psi = 0$; cf. the discussion of conditions for incompressibility in Sec. 13.6. [The near-zone equation $\nabla^2\psi = 0$ is analogous to $\nabla^2\Phi = 0$ for the Newtonian gravitational potential in the weak-gravity near zone of a gravitational-wave source (Sec. 27.5.2).

The general monopolar (spherical) solution to $\nabla^2\psi = 0$ is

$$\psi = \frac{A(t)}{r} + B(t) \ . \tag{16.71}$$

Matching the fluid's radial velocity $v = \partial\psi/\partial r = -A/r^2$ at $r = a$ to the ball's radial velocity $\dot{\xi}$, we obtain

$$A(t) = -a^2\dot{\xi}(t) \ . \tag{16.72}$$

---
[6]Our treatment is based on Burke (1970).

From the point of view of near-zone physics there is no mechanism for generating a nonzero spatially constant term $B(t)$ in ψ [Eq. (16.71)], so if one were unaware of the emitted waves and their action back on the source, one would be inclined to set $B(t)$ to zero. [This is analogous to a Newtonian physicist, who would be inclined to write the quadrupolar contribution to an axisymmetric source's external gravitational field in the form $\Phi = P_2(\cos\theta)[A(t)r^{-3} + B(t)r^2]$ and then, being unaware of gravitational waves and their action back on the source, would set $B(t)$ to zero.] Taking this near-zone viewpoint, with $B = 0$, we infer that the fluid's pressure perturbation acting on the ball's surface is

$$\delta P = -\rho\frac{\partial\psi(a,t)}{\partial t} = -\rho\frac{\dot{A}}{a} = \rho a\ddot{\xi} \tag{16.73}$$

[Eqs. (16.51)) and (16.72)].

The motion $\xi(t)$ of the ball's surface is controlled by the elastic restoring forces in its interior and the fluid pressure perturbation δP on its surface. In the absence of δP the surface would oscillate sinusoidally with some angular frequency ω_o, so $\ddot{\xi} + \omega_o^2\xi = 0$. The pressure will modify this to

$$m(\ddot{\xi} + \omega_o^2\xi) = -4\pi a^2\delta P , \tag{16.74}$$

where m is an effective mass, roughly equal to the ball's true mass, and the right hand side is the integral of the radial component of the pressure perturbation force over the sphere's surface. Inserting the near-zone viewpoint's pressure perturbation (16.73), we obtain

$$(m + 4\pi a^3\rho)\ddot{\xi} + m\omega_o^2\xi = 0 . \tag{16.75}$$

Evidently, the fluid increases the ball's effective inertial mass (it *loads* additional mass onto the ball), and thereby reduces its frequency of oscillation to

$$\omega = \frac{\omega_o}{\sqrt{1 + \kappa}} , \quad \text{where } \kappa = \frac{4\pi a^3\rho}{m} \tag{16.76}$$

is a measure of the coupling strength between the ball and the fluid. In terms of this loaded frequency, the equation of motion becomes

$$\ddot{\xi} + \omega^2\xi = 0 . \tag{16.77}$$

This near-zone viewpoint is not quite correct, just as the standard Newtonian viewpoint is not quite correct for the near-zone gravity of a gravitational-wave source (Sec. 27.5.3). To improve on this viewpoint, we temporarily move out into the wave zone and identify the general, outgoing-wave solution to the sound wave equation,

$$\psi = \frac{f(t - \epsilon r/c)}{r} \tag{16.78}$$

[Eq. (16.64)]. Here f is a function to be determined by matching to the near zone, and ϵ is a parameter that has been inserted to trace the influence of the outgoing-wave boundary condition. For outgoing waves (the real, physical, situation), $\epsilon = +1$; if the waves were ingoing, we would have $\epsilon = -1$.

This wave-zone solution remains valid down into the near zone. In the near zone we can perform a slow-motion expansion to bring it into the same form as the near-zone velocity potential (16.71):

$$\psi = \frac{f(t)}{r} - \epsilon\frac{\dot{f}(t)}{C} + \dots .$$
(16.79)

The second term is sensitive to whether the waves are outgoing or ingoing and thus must ultimately be responsible for the radiation reaction force that acts back on the oscillating ball; for this reason we will call it the *radiation-reaction potential.*

Equating the first term of this ψ to the first term of (16.71) and using the value (16.72) of $A(t)$ obtained by matching the fluid velocity to the ball velocity, we obtain

$$f(t) = A(t) = -a^2\dot{\xi}(t) .$$
(16.80)

This equation tells us that the wave field $f(t - r/C)/r$ generated by the ball's surface displacement $\xi(t)$ is given by $\psi = -a^2\dot{\xi}(t - r/C)/r$ [Eq. (16.66)] — the result we derived more quickly in the previous section. *We can regard Eq. (16.80) as matching the near-zone solution outward onto the wave-zone solution to determine the wave field as a function of the source's motion.*

Equating the second term of Eq. (16.79) to the second term of the near-zone velocity potential (16.71) we obtain

$$B(t) = -\epsilon\frac{\dot{f}(t)}{C} = \epsilon\frac{a^2}{C}\ddot{\xi}(t) .$$
(16.81)

This is the term in the near-zone velocity potential $\psi = A/r + B$ that will be responsible for radiation reaction. *We can regard this radiation reaction potential $\psi^{\mathrm{RR}} = B(t)$ as having been generated by matching the wave zone's outgoing ($\epsilon = +1$) or ingoing ($\epsilon = -1$) wave field back into the near zone.* [A similar matching analysis by Burke (1971) led him to the gravitational radiation reaction potential (27.62).]

This pair of matchings, outward then inward (Fig. 16.11), is a special, almost trivial example of the technique of *matched asymptotic expansions* — a technique developed by applied mathematicians to deal with much more complicated matching problems than this one (see e.g. Cole, 1968).

The radiation-reaction potential $\psi^{\mathrm{RR}} = B(t) = \epsilon(a^2/C)\ddot{\xi}(t)$ gives rise to a radiation-reaction contribution to the pressure on the ball's surface $\delta P^{\mathrm{RR}} = -\rho\dot{\psi}^{\mathrm{RR}} = -\epsilon(\rho a^2/C)\dddot{\xi}$. Inserting this into the equation of motion (16.74) along with the loading pressure (16.73) and performing the same algebra as before, we get the following radiation-reaction-modified form of Eq. (16.77):

$$\boxed{\ddot{\xi} + \omega^2\xi = \epsilon\tau\dddot{\xi}} , \quad \text{where } \tau = \frac{\kappa}{1 + \kappa}\frac{a}{C}$$
(16.82)

is less than the fluid's sound travel time to cross the ball's radius, a/C. The term $\epsilon\tau\dddot{\xi}$ in the equation of motion is the ball's *radiation-reaction acceleration,* as we see from the fact that it would change sign if we switched from outgoing waves, $\epsilon = +1$, to ingoing waves, $\epsilon = -1$.

In the absence of radiation reaction, the ball's surface oscillates sinusoidally in time, $\xi = e^{\pm i\omega t}$. The radiation reaction term produces a weak damping of these oscillations:

$$\boxed{\xi \propto e^{\pm i\omega t}e^{-\sigma t} , \quad \text{where } \sigma = \frac{1}{2}\epsilon(\omega\tau)\omega}$$
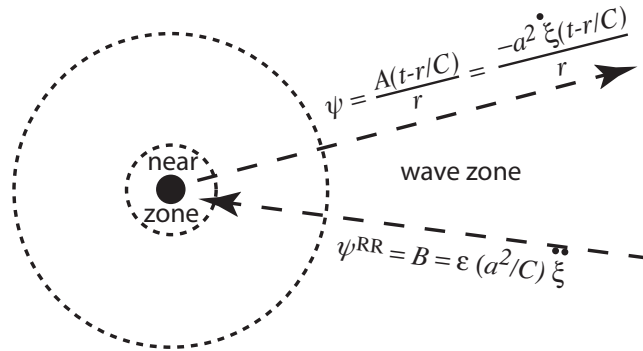(16.83)

Fig. 16.11: Matched asymptotic expansions for an oscillating ball emitting sound waves. The near-zone expansion feeds the radiation field $\psi = \frac{1}{r}A(t - r/C) = -\frac{1}{r}a^2\dot{\xi}(t - r/C)$ into the wave zone. The wave-zone expansion then feeds the radiation-reaction field $\psi^{\mathrm{RR}} = B = \epsilon(a^2/C)\dddot{\xi}$ back into the near zone, where it produces the radiation-reaction pressure $\delta P^{\mathrm{RR}} = -\rho\dot{\psi}^{\mathrm{RR}}$ on the ball's surface.

is the radiation-reaction-induced damping rate (with $\epsilon = +1$). Note that in order of magnitude the ratio of the damping rate to the oscillation frequency is $\sigma/\omega = \omega\tau \lesssim \omega a/C = a/\lambda$, which is small compared to unity by virtue of the slow-motion assumption. If the waves were ingoing rather than outgoing, $\epsilon = -1$, the fluid's oscillations would grow. In either case, outgoing waves or ingoing waves, the radiation reaction force removes energy from the ball or adds it at the same rate as the sound waves carry energy off or bring it in. The total energy, wave plus ball, is conserved.

Expression (16.83) is two linearly independent solutions to the equation of motion (16.82), one with the sign $+$ and the other $-$. Since this equation of motion has been made third order by the radiation-reaction term, there must be a third independent solution. It is easy to see that, up to a tiny fractional correction, that third solution is

$$\xi \propto e^{\epsilon t/\tau} \ . \tag{16.84}$$

For outgoing waves, $\epsilon = +1$, this solution grows exponentially in time, on an extremely rapid timescale $\tau \lesssim a/C$; it is called a *runaway solution.*

Such runaway solutions are ubiquitous in equations of motion with radiation reaction. For example, a computation of the electromagnetic radiation reaction on a small, classical, electrically charged, spherical particle gives the Abraham-Lorentz equation of motion

$$m(\ddot{\mathbf{x}} - \tau\dddot{\mathbf{x}}) = \mathbf{F}_{\mathrm{ext}} \tag{16.85}$$

(Rorlich 1965; Sec. 16.2 of Jackson 1999). Here $\mathbf{x}(t)$ is the the particle's world line, $\mathbf{F}_{\mathrm{ext}}$ is the external force that causes the particle to accelerate, and the particle's inertial mass m includes an electrostatic contribution analogous to $4\pi a^3\rho$ in our fluid problem. The timescale τ, like that in our fluid problem, is very short, and when the external force is absent, there is a runaway solution $\mathbf{x} \propto e^{t/\tau}$.

Much human heat and confusion were generated, in the the early and mid 20th century, over these runaway solutions (see, e.g., Rorlich 1965). For our simple model problem, there

need be little heat or confusion. One can easily verify that the runaway solution (16.84) violates the slow-motion assumption $a/\lambda \ll 1$ that underlies our derivation of the radiation reaction acceleration. It therefore is a spurious solution.

Our model problem is sufficiently simple that one can dig deeper into it and learn that the runaway solution arises from the slow-motion approximation trying to reproduce a genuine, rapidly damped solution and getting the sign of the damping wrong (Ex. 16.16 and Burke 1970).

<div align="center">****************************</div>

EXERCISES

Exercise 16.15 *Problem: Energy Conservation for Radially Oscillating Ball Plus Sound Waves*
For the radially oscillating ball as analyzed in Sec. 16.5.3, verify that the radiation reaction acceleration removes energy from the ball, plus the fluid loaded onto it, at the same rate as the sound waves carry energy away. See Ex. 27.11 for the analogous gravitational-wave result.

Exercise 16.16 *Problem: Radiation Reaction Without the Slow Motion Approximation*
Redo the computation of radiation reaction for a radially oscillating ball immersed in a fluid, without imposing the slow-motion assumption and approximation. Thereby obtain the following coupled equations for the radial displacement $\xi(t)$ of the ball's surface and the function $\Phi(t) \equiv a^{-2} f(t - \epsilon a/C)$, where $\psi = r^{-1} f(t - \epsilon r/C)$ is the sound-wave field:

$$\ddot{\xi} + \omega_o^2 \xi = \kappa \dot{\Phi} , \quad \dot{\xi} = -\Phi - \epsilon(a/C)\dot{\Phi} . \tag{16.86}$$

Show that in the slow-motion regime, this equation of motion has two weakly damped solutions of the same form (16.83) as we derived using the slow-motion approximation, and one rapidly damped solution $\xi \propto \exp(-\epsilon \kappa t/\tau)$. Burke (1970) shows that the runaway solution (16.84) obtained using the slow-motion approximation is caused by that approximation's futile attempt to reproduce this genuine, rapidly damped solution.

Exercise 16.17 *Problem: Sound Waves from a Ball Undergoing Quadrupolar Oscillations*
Repeat the analysis of sound wave emission, radiation reaction, and energy conservation, as given in Sec. 16.5.3 and Ex. 16.15, for axisymmetric, quadrupolar oscillations of an elastic ball, $r_{\text{ball}} = a + \xi(t) P_2(\cos\theta)$.
Comment: Since the lowest multipolar order for gravitational waves is quadrupolar, this exercise is closer to the analogous problem of gravitational wave emission than the monopolar analysis in the text.
Hint: If ω is the frequency of the ball's oscillations, then the sound waves have the form

$$\psi = K \Re \left[e^{-i\omega t} \left(\frac{n_2(\omega r/C) - i\epsilon j_2(\omega r/C)}{r} \right) \right] , \tag{16.87}$$

where K is a constant, $\Re(X)$ is the real part of X, ϵ is $+1$ for outgoing waves and -1 for ingoing waves, and j_2 and n_2 are the spherical Bessel and spherical Neuman functions of order 2. In the distant wave zone, $x \equiv \omega r/C \gg 1$,

$$n_2(x) - i\epsilon j_2(x) = \frac{e^{i\epsilon x}}{x} \; ; \tag{16.88}$$

in the near zone $x = \omega r/C \ll 1$,

$$n_2(x) = -\frac{3}{x^3}\left(1 \,\&\, x^2 \,\&\, x^4 \,\&\, \ldots\right) \;, \quad j_2(x) = \frac{x^2}{15}\left(1 \,\&\, x^2 \,\&\, x^4 \,\&\, \ldots\right) \;. \tag{16.89}$$

Here "$\& \; x^n$" means "$+$ (some constant)x^n".

$$************************$$

Bibliographic Note

For physical insight into waves in fluids, we recommend the movies discussed in Box 16.2. Among fluid dynamics textbooks, those that we most like for their treatment of waves are Acheson (1990), Lautrup (2005), and Kundu, Cohen and Dowling (2012). For greater depth and detail, we recommend two books solely devoted to waves: Lighthill (1978) and Whitham (1974).

For Rossby waves (which are omitted from most fluid dynamics texts), we recommend the very physical descriptions and analyses in Tritton (1977). For solitons, we like Chap. 17 of Whitham (1974); also Drazin and Johnson (1989), which focuses on the mathematics of the Korteweg de Vries equation; Ablowitz (2011), which treats the mathematics of solitons plus applications to fluids and nonlinear optics; and Dauxois and Payrard (2006), which treats the mathematics and applications to plasmas and condensed matter physics.

The mathematics of matched asymptotic expansions is nicely developed by Cole (1974) and by Lagerstrom (1988). Radiation reaction in wave emission is not treated pedagogically in any textbook that we know of except ours; for pedagogical original literature, we like Burke (1970).

Bibliography

Ablowitz, Mark J. 2011. *Nonlinear Dispersive Waves: Asymptotic Analysis and Solitons*, Cambridge: Cambridge University Press.

Acheson, D. J. 1990. *Elementary Fluid Dynamics*, Oxford: Clarendon Press.

Bryson, A.E. 1964. *Waves in Fluids*, a movie (National Committee for Fluid Mechanics Films); available at `http://web.mit.edu/hml/ncfmf.html` .

Box 16.5
Important Concepts in Chapter 16

- Gravity waves on water and other liquids, Sec. 16.2

    - Deep water waves and shallow water waves, Secs. 16.2.1, 16.2.2
    - Nonlinear shallow water waves, Box 16.3
    - Tsunamis, Ex. 16.6
    - Dispersion, Sec. 16.3.1
    - Steepening due to nonlinear effects, Sec. 16.3.1, Fig. 16.4
    - Solitons or solitary waves; nonlinear steepening balances dispersion, Sec. 16.3
    - Korteweg-deVries equation, Secs. 16.3.1–16.3.4

- Surface tension and its stress tensor, Box 16.4

    - Capillary waves, Sec. 16.2.3

- Rossby Waves in a Rotating Fluid, Sec. 16.4

- Sound waves in fluids and gases, Sec. 16.5

    - Sound wave generation in slow-motion approximation: power proportional to squared time derivative of monopole moment, Sec. 16.5.2
    - Decibel, Sec. 16.5.2
    - Matched asymptotic expansions, Sec. 16.5.3
    - Radiation reaction force; runaway solution as a spurious solution that violates the slow-motion approximation used to derive it, Sec. 16.5.3

Burke, W. W. 1970. "Runaway solutions: remarks on the asymptotic theory of radiation damping," *Phys. Rev. A* **2**, 1501–1505.G

Cole, J. 1974. *Perturbation Methods in Applied Mathematics*, Waltham Mass: Blaisdell.

Chelton, D.B. and Schlax, M.G. 1996. "Global observations of oceanic Rossby waves", *Science*, **272**, 234.

Dauxois, Thierry, and Peyrard, Michel. 2006. *Physics of Solitons*, Cambridge: Cambridge University Press.

Drazin, P. G., and Johnson, R. S. 1989. *Solitons: An Introduction*, Cambridge: Cambridge University Press

Fultz, D. 1969. *Rotating Flows*, a movie (National Committee for Fluid Mechanics Films); available at `http://web.mit.edu/hml/ncfmf.html` .

Gill, A. E. 1982. *Atmosphere Ocean Dynamics*, New York: Academic Press.

Greenspan, H. P. 1973. *The Theory of Rotating Fluids*, Cambridge: Cambridge University Press.

Jackson, J. D. 1999. *Classical Electrodynamics*, third edition, New York: Wiley.

Kundu, Pijush K., Cohen, Ira M., and Dowling, David R. 2012. *Fluid Mechanics*, fifth edition, New York: Academic Press.

Lagerstrom, P. 1988. *Matched Asymptotic Expansions: Ideas and Techniques*, Berlin: Springer-Verlag.

Landau, L. D. and Lifshitz, E. M. 1959. *Fluid Dynamics*, Oxford: Pergamon.

Lautrup, B. 2005. *Physics of Continuous Matter*, Bristol UK: Institute of Physics.

Libbrecht, K. G. & Woodard, M. F. 1991. *Science*, **253**, 152.

Lighthill, M. J. 1978. *Waves in Fluids*, Cambridge: Cambridge University Press.

Pellew, A. and Southwell, R. V. 1940. *Proceedings of the Royal Society*, **A176**, 312.

Rorlich, F. 1965. *Classical Charged Particles*, Reading Mass: Addison Wesley.

Scott-Russell, J. 1844. *Proc. Roy. Soc. Edinburgh*, 319 (1844).

Tritton, D. J. 1987. *Physical Fluid Dynamics*, Oxford: Oxford Science Publications.

Whitham, G. B. 1974. *Linear and Non-Linear Waves*, New York: Wiley.